

7-26-2018

Data-Based Nonlinear Model Identification in Economic Model Predictive Control

Laura Giuliani

University of Study of L'Aquila

Helen Durand

Wayne State University, helen.durand@wayne.edu

Follow this and additional works at: https://digitalcommons.wayne.edu/cems_eng_frp



Part of the [Controls and Control Theory Commons](#), [Industrial Engineering Commons](#), [Operational Research Commons](#), and the [Process Control and Systems Commons](#)

Recommended Citation

Giuliani, L. and Durand, H., "Data-Based Nonlinear Model Identification in Economic Model Predictive Control," *Smart and Sustainable Manufacturing Systems*, Vol. 2, No. 2, 2018, pp. 61–109, <https://doi.org/10.1520/SSMS20180025>. ISSN 2520-6478

This Article is brought to you for free and open access by the Chemical Engineering and Materials Science at DigitalCommons@WayneState. It has been accepted for inclusion in Chemical Engineering and Materials Science Faculty Research Publications by an authorized administrator of DigitalCommons@WayneState.

Laura Giuliani¹ and Helen Durand²

Data-Based Nonlinear Model Identification in Economic Model Predictive Control

Reference

Giuliani, L. and Durand, H., "Data-Based Nonlinear Model Identification in Economic Model Predictive Control," *Smart and Sustainable Manufacturing Systems*, Vol. 2, No. 2, 2018, pp. 61–109, <https://doi.org/10.1520/SSMS20180025>. ISSN 2520-6478

ABSTRACT

Many chemical/petrochemical processes in industry are not completely modeled from a first-principles perspective because of the complexity of the underlying physico-chemical phenomena and the cost of obtaining more accurate, physically relevant models. System identification methods have been utilized successfully for developing empirical, though not necessarily physical, models for advanced model-based control designs such as model predictive control (MPC) for decades. However, a fairly recent development in MPC is economic model predictive control (EMPC), which is an MPC formulated with an economics-based objective function that may operate a process in a dynamic (i.e., off steady-state) fashion, in which case the details of the process model become important for obtaining sufficiently accurate state predictions away from the steady-state, and the physics and chemistry of the process become important for developing meaningful profit-based objective functions and safety-critical constraints. Therefore, methods must be developed for obtaining physically relevant models from data for EMPC design. While the literature regarding developing models from data has rapidly expanded in recent years, many new techniques require a model structure to be assumed *a priori*, to which the data is then fit. However, from the perspective of developing a physically meaningful model for a chemical process, it is often not obvious what structure to assume for the model, especially considering the often complex nonlinearities characteristic of chemical processes (e.g., in reaction rate laws). In this work, we suggest that the controller itself may facilitate the identification of physically relevant models online from process operating data by forcing the process state to nonroutine operating conditions

Manuscript received March 19, 2018; accepted for publication June 4, 2018; published online July 26, 2018.

¹ Department of Industrial and Information Engineering and Economics, University of Study of L'Aquila, Via Giovanni Gronchi 18 - Zona industriale di Pile, L'Aquila 67100, Italy

² Department of Chemical Engineering and Materials Science, Wayne State University, 5050 Anthony Wayne Dr., Detroit, MI 48202, USA (Corresponding author), e-mail: helen.durand@wayne.edu,  <https://orcid.org/0000-0002-2857-4781>

for short periods of time to obtain data that can aid in selecting model structures believed to have physical significance for the process and, subsequently, identifying their parameters. Specifically, we develop EMPC designs for which the objective function and constraints can be changed for short periods of time to obtain data to aid in model structure selection. For one of the developed designs, we incorporate Lyapunov-based stability constraints that allow closed-loop stability and recursive feasibility to be proven even as the online “experiments” are performed. This new design is applied to a chemical process example to demonstrate its potential to facilitate physics-based model identification without loss of closed-loop stability. This work therefore reverses a question that has been of interest to the control community (i.e., how new techniques for developing models from data can be useful for control of chemical processes) to ask how control may be utilized to impact the use of these techniques for the identification of physically relevant process dynamic models that can aid in improving process operation and control for economic and safety purposes.

Keywords

economic model predictive control, nonlinear model identification, regression

Introduction

Many industrial chemical processes are complex or poorly understood; however, to control such processes with advanced model-based control designs like model predictive control (MPC) [1–3], sufficiently accurate process models are required [4]. There is a significant incentive for companies to employ MPC for certain processes because it is able to determine control actions that are optimal with respect to the objective function of the controller (which in industrial applications of MPC has been a quadratic objective function with its minimum at a process steady-state) and that cause constraints to be met. To facilitate the use of MPC in cases where process models are not available, system identification techniques [5–8] can be employed to develop process models.

A variety of system identification methods exist, some of which identify linear process models [9] (which often provide reasonably accurate state predictions for an MPC because chemical processes have traditionally been operated around a process steady-state where a linear model can sufficiently approximate the nonlinear process dynamics), whereas others can identify nonlinear models [5]. System identification techniques can be classified into input–output [5,10] and state-space [7,11] methods, depending on whether they produce models relating the inputs and outputs of the process, or instead models reflecting the dynamics of process states. A characteristic of system identification techniques is that a structure for the process model must be chosen before the method can be used (e.g., before the MOESP [9,12,13] method can be used, it must be assumed that the process dynamics can be adequately characterized by a linear state-space empirical model). Many system identification techniques require a relatively specific structure for the model (e.g., a linear or polynomial structure) that is not highly conducive to being able to extract physically meaningful dynamic models (e.g., conservation equations) from the techniques. Once this structure is selected, it may be assumed that all coefficients of that model can exist (i.e., the model identification problem becomes a data-fitting problem, rather than an

attempt to determine which terms most represent the underlying dynamics; indeed, it is not possible to attempt to determine which terms most represent the underlying dynamics if the selected model structure is not representative of the underlying dynamics). However, methods for extracting dynamic models from data such as those based on symbolic and sparse regression techniques in Refs. [14] and [15], respectively, have examined how models containing only a subset of terms available to the model identification algorithm might be obtained. In recent years, there has been a growing interest in machine learning [16] and data science [17], which are related to the solutions of a variety of model identification problems. Various MPC designs have been developed that can take advantage of aspects of machine learning such as support vector machines [18], reinforcement learning [19], neural networks [20–22], and sparse regression [23]. Model reduction techniques that support MPC design have included the naive elastic net technique with orthogonal decomposition [24] and clustering with dynamic mode decomposition with control [25], which have been demonstrated to have applications for the hydraulic fracturing process.

The need to obtain physics-based models of chemical processes from operating data is growing as there are greater pushes toward smart/next-generation manufacturing techniques that seek to streamline process operation and control [26,27]. From an operational standpoint, physics-based process models can improve an engineer's understanding of the dynamics of a process to aid in trouble-shooting and therefore to enhance profits. They may also aid in improvements to both process operational and maintenance safety by giving employees a better understanding of how the process behaves under different conditions. On the control side, physically meaningful models are important for the design of advanced MPC-type controllers such as economic model predictive controllers (EMPC's) [28–30]. EMPC is an MPC design that is not required to have the minimum value of the objective function at a process steady-state (it allows for general economics-based objective functions in MPC so that the control actions are economically optimal with respect to the objective function, given the constraints). EMPC may operate a process in a time-varying fashion, rather than driving the process state to a steady-state. This introduces new challenges related to the practical design of these controllers that have not been encountered before with traditional tracking MPC designs. For example, nonlinearities in the dynamics may become important for making state predictions when the EMPC operates a process in a time-varying fashion, and the traditional linear empirical models utilized in industry may only provide reasonably good state predictions in a neighborhood of the origin, thereby potentially limiting the economic performance of a process operated under an EMPC using a linear empirical model compared to one that uses a more accurate nonlinear model [31,32]. Furthermore, the constraints and objective function of EMPC are often physics-based (e.g., an economics-based objective function may be related to process behavior known to enhance or detract from profits, and physically meaningful constraints, such as those related to safety [33], may be important to prevent the potentially off steady-state operation of the EMPC from leading to dangerous operating conditions).

The traditional technique used for obtaining physically meaningful models of processes where dynamics are not known has been to perform experiments in a laboratory setting. In these cases, specific variables are often fixed so that the impacts on measured states of changing other variables can be observed. Online model identification is preferable to extensive laboratory testing given the cost of performing many experiments, but model identification techniques may require that the data to be used for model identification is adequate for the algorithm being utilized to derive a model. Furthermore, it can be

desirable to check how well an identified model fits data that was not utilized to develop it to be sure that the identified model has good predictive performance.

Experimentation, developing appropriate data for model identification techniques, and developing nontraining data to use in model validation all require methods for changing the process inputs in well-characterized and desired ways, though not for long periods of time. MPC's have long been utilized to manipulate process inputs; EMPC presents even greater flexibility in the objective function and constraints than traditional tracking MPC for adjusting the process inputs in desired ways and also has the ability to move the process state throughout an operating region rather than forcing it to a steady-state. Motivated by these considerations, in this work, we develop EMPC designs that can be utilized to seek to obtain specific process data for short periods of time to aid in obtaining physically meaningful process models from data online to use in updating the EMPC's (including the model, constraints, and objective function) so that their design becomes more conducive to achieving operational economic and safety goals. We present an example formulation of the proposed controller with Lyapunov-based stability constraints that can achieve flexibility in manipulating the process states while maintaining closed-loop stability and recursive feasibility, even in the presence of disturbances. A chemical process example is utilized to demonstrate the potential benefits of utilizing an EMPC for online model identification and online EMPC design. This work extends that in [34].

Preliminaries

NOTATION

The Euclidean norm and transpose of a vector x are denoted by $|x|$ and x^T , respectively. The function $\alpha(\cdot): [0, a) \rightarrow [0, \infty)$ belongs to class \mathcal{K} if it is strictly increasing and $\alpha(0) = 0$. For a sufficiently smooth, positive definite function V , we define $\Omega_\rho := \{x \in \mathbb{R}^n : V(x) \leq \rho\}$. Set subtraction is signified by “/” (i.e., $x \in A/B := \{x \in A : x \notin B\}$). An $n \times n$ matrix with the entries of the vector $x \in \mathbb{R}^n$ on its diagonal is denoted by $\text{diag}(x)$. The floor function $\lfloor \cdot \rfloor$ returns the largest integer less than its argument.

CLASS OF SYSTEMS

The class of nonlinear systems considered is the following:

$$\dot{x}(t) = f(x(t), u(t), w(t)) \quad (1)$$

where f is a nonlinear locally Lipschitz vector function of the state vector $x \in X \subset \mathbb{R}^n$, the manipulated input vector $u \in \mathbb{R}^m$, and the disturbance vector $w \in \mathbb{R}^l$, where X represents the set where the state is constrained. The control action is constrained in $U := \{u \in \mathbb{R}^m : u_i^{\min} \leq u_i \leq u_i^{\max}, i = 1, \dots, m\}$, while the noise is bounded in $W \subset \mathbb{R}^l$ ($w \in W := \{w \in \mathbb{R}^l : |w(t)| \leq \Theta, \Theta > 0\}$). We will refer to Eq 1 as the nominal system when $w(t) \equiv 0$. The origin of the nominal nonlinear system is considered to be the equilibrium point (i.e., $f(0, 0, 0) = 0$). The state is measured at each sampling time $t_k = k\Delta$ where $k = 0, 1, \dots$, and Δ is the sampling period. We restrict the class of nonlinear systems considered to those for which there exists an explicit stabilizing Lyapunov-based controller $h(x)$ that is locally Lipschitz and is able to render the origin asymptotically stable in the sense that there exists a sufficiently smooth Lyapunov function $V: \mathbb{R}^n \rightarrow \mathbb{R}_+$ such that:

$$\alpha_1(|x|) \leq V(x) \leq \alpha_2(|x|) \quad (2)$$

$$\frac{\partial V(x)}{\partial x} f(x, h(x), 0) \leq -\alpha_3(|x|) \quad (3)$$

$$\left| \frac{\partial V(x)}{\partial x} \right| \leq \alpha_4(|x|) \quad (4)$$

$$h(x) \in U \quad (5)$$

for all $x \in D \subset \mathbb{R}^n$, where D is an open neighborhood of the origin and the $\alpha_i(\cdot)$, $i = 1, 2, 3, 4$, are functions of class \mathcal{K} . We define $\Omega_\rho \subset D$ to be the stability region of the nominal closed-loop system under the controller $h(x)$ and require that it be chosen such that $x \in X$, $\forall x \in \Omega_\rho$. Because V is a sufficiently smooth function and f is locally Lipschitz, the following inequalities hold:

$$|f(x_1, u, w) - f(x_2, u, 0)| \leq L_x |x_1 - x_2| + L_w |w| \quad (6)$$

$$\left| \frac{\partial V(x_1)}{\partial x} f(x_1, u, w) - \frac{\partial V(x_2)}{\partial x} f(x_2, u, 0) \right| \leq L'_x |x_1 - x_2| + L'_w |w| \quad (7)$$

$\forall x_1, x_2 \in \Omega_\rho$, $u \in U$, and $w \in W$, where L_x, L'_x, L_w , and L'_w are positive constants. Moreover, there exists $M > 0$ that is bounded such that

$$|f(x, u, w)| \leq M \quad (8)$$

$\forall x \in \Omega_\rho$, $u \in U$, and $w \in W$ because $f(\cdot, \cdot, \cdot)$ is a locally Lipschitz vector function.

In this work, we assume that the nonlinear model of Eq 1 is not available, so we instead develop an empirical model that can have a general nonlinear form as follows:

$$\dot{x}(t) = f_{NL}(x(t), u(t)) \quad (9)$$

where f_{NL} is a locally Lipschitz nonlinear vector function of the state $x \in \mathbb{R}^n$ and the input $u \in \mathbb{R}^m$ with $f_{NL}(0, 0) = 0$. We consider empirical models for which the origin can be rendered asymptotically stable by a locally Lipschitz explicit stabilizing controller $h_{NL}(x)$ in the sense that

$$\hat{\alpha}_1(|x|) \leq \hat{V}(x) \leq \hat{\alpha}_2(|x|) \quad (10)$$

$$\frac{\partial \hat{V}(x)}{\partial x} f_{NL}(x, h_{NL}(x)) \leq -\hat{\alpha}_3(|x|) \quad (11)$$

$$\left| \frac{\partial \hat{V}(x)}{\partial x} \right| \leq \hat{\alpha}_4(|x|) \quad (12)$$

$$h_{NL}(x) \in U \quad (13)$$

for all $x \in D_{NL}$, where $\hat{V}: \mathbb{R}^n \rightarrow \mathbb{R}_+$ is a sufficiently smooth Lyapunov function and $\hat{\alpha}_i$, $i = 1, 2, 3, 4$ are class \mathcal{K} functions. We define $\Omega_\rho \subset D_{NL}$ (chosen such that $x \in X$, $\forall x \in \Omega_\rho$) as the stability region of the system of Eq 9. There exist $M_L > 0$ and $L_L > 0$ such that

$$|f_{NL}(x, u)| \leq M_L \quad (14)$$

$$\left| \frac{\partial \hat{V}(x_1)}{\partial x} f_{NL}(x_1, u) - \frac{\partial \hat{V}(x_2)}{\partial x} f_{NL}(x_2, u) \right| \leq L_L |x_1 - x_2| \quad (15)$$

$\forall x, x_1, x_2 \in \Omega_\beta$ and $u \in U$. Furthermore, because f is a locally Lipschitz function of its arguments, we can also write the following $\forall x_1, x_2 \in \Omega_\beta$, $u \in U$, and $w \in W$, and \bar{L}_x , \bar{L}_w , \bar{L}'_x , and \bar{L}'_w as positive constants:

$$|f(x_1, u, w) - f(x_2, u, 0)| \leq \bar{L}_x |x_1 - x_2| + \bar{L}_w |w| \quad (16)$$

$$\left| \frac{\partial \hat{V}(x_1)}{\partial x} f(x_1, u, w) - \frac{\partial \hat{V}(x_2)}{\partial x} f(x_2, u, 0) \right| \leq \bar{L}'_x |x_1 - x_2| + \bar{L}'_w |w| \quad (17)$$

Remark 1. We assume full state feedback, and therefore do not consider the case where a physics-based empirical model to be developed must model or account for the effects of unmeasured states.

EMPC

EMPC is a control design that determines control actions to apply to a process by solving an optimization problem of the following form:

$$\min_{u(t) \in \mathcal{S}(\Delta)} \int_{t_k}^{t_{k+N}} L_e(\tilde{x}(\tau), u(\tau)) \, d\tau \quad (18)$$

$$\text{s.t. } \dot{\tilde{x}}(t) = f(\tilde{x}(t), u(t), 0) \quad (19)$$

$$\tilde{x}(t_k) = x(t_k) \quad (20)$$

$$\tilde{x}(t) \in X, \forall t \in [t_k, t_{k+N}) \quad (21)$$

$$u(t) \in U, \forall t \in [t_k, t_{k+N}) \quad (22)$$

where the stage cost $L_e(\tilde{x}, u)$ is minimized (Eq 18), subject to a nominal system model (Eq 19) and the initial condition in Eq 20 that sets the predicted state (\tilde{x}) equal to the measured state at the sampling time. \tilde{x} and the input u are bounded (Eqs 21 and 22). The notation $u(t) \in \mathcal{S}(\Delta)$ signifies that the inputs are piecewise constant over the prediction horizon comprised of N sampling periods of length Δ . It is noted that the nominal nonlinear dynamic model of Eq 1 is used in Eq 19 (i.e., this is not an empirical model) for consistency with the majority of the EMPC literature, which has, in general, not considered empirical models (some exceptions include Refs. [31,32,35–38]). The use of an empirical model in the EMPC development in this work will be clarified in what follows.

LYAPUNOV-BASED EMPC

Lyapunov-based EMPC (LEMPC) [39] is formulated as follows:

$$\min_{u(t) \in \mathcal{S}(\Delta)} \int_{t_k}^{t_{k+N}} L_e(\tilde{x}(\tau), u(\tau)) \, d\tau \quad (23)$$

$$\text{s.t. } \dot{\tilde{x}}(t) = f(\tilde{x}(t), u(t), 0) \quad (24)$$

$$\tilde{x}(t_k) = x(t_k) \quad (25)$$

$$\tilde{x}(t) \in X, \forall t \in [t_k, t_{k+N}) \quad (26)$$

$$u(t) \in U, \forall t \in [t_k, t_{k+N}) \quad (27)$$

$$V(\tilde{x}(t)) \leq \rho_e, \forall t \in [t_k, t_{k+N}), \text{ if } x(t_k) \in \Omega_{\rho_e} \quad (28)$$

$$\begin{aligned} & \frac{\partial V(x(t_k))}{\partial x} f(x(t_k), u(t_k), 0) \\ & \leq \frac{\partial V(x(t_k))}{\partial x} f(x(t_k), h(x(t_k)), 0) \text{ if } x(t_k) \notin \Omega_{\rho_e} \end{aligned} \quad (29)$$

The notation in Eqs 23–29 is like that in Eqs 18–22 but with Eqs 28 and 29 added to ensure that the closed-loop state cannot leave Ω_{ρ} . Eq 28 requires that the predicted state is contained in $\Omega_{\rho_e} \subset \Omega_{\rho}$ throughout the prediction horizon if $x(t_k) \in \Omega_{\rho_e}$. Eq 29 is applied when $x(t_k) \notin \Omega_{\rho_e}$ and causes the LEMPC to compute control actions that will drive the closed-loop state into Ω_{ρ_e} in finite time.

Data-Gathering EMPC Design

EMPC may require an understanding of the process dynamics for developing an appropriate economics-based objective function and meaningful constraints. It would be expected that system identification techniques would be more preferable to use for obtaining dynamic models for EMPC than first-principles modeling for many large-scale or complex chemical processes. However, though empirical models have the potential to enable sufficiently accurate state predictions by the controller, they may not aid in the development of constraints or objective functions that are reflective of the physics and chemistry of the process. Therefore, in the following sections, we will develop a class of EMPC formulations and their implementation strategy that can aid in obtaining data for developing and validating empirical models with potentially physically meaningful terms.

MOTIVATING CONSIDERATIONS

A hurdle in obtaining a physics-based model from data can be obtaining good data for using the chosen identification technique or validating the model obtained from it. For example, an MPC will operate a process at steady-state, in which case the changes in states and inputs over time would be expected to be relatively minimal. An EMPC may also find a steady-state to be an economically optimal operating point with respect to the objective function and constraints. As a result, the routine operating data would be expected to be approximately the same for extended periods of time and may not aid in utilizing certain methods for getting models from data or in having different data available with which to validate a model than was used to identify it.

A second hurdle in obtaining a physics-based model can be selecting physically meaningful model structures with which to fit the data. For example, consider a novel technique for developing dynamic models from data in Ref. [15]. In this work, it is proposed that a dynamic model with potentially physically relevant terms may be developed from data through a sparse regression technique. A large number of terms can initially be postulated

that may potentially be present in the model, and sparse regression is utilized to attempt to identify coefficients for the postulated terms that trade off between fitting the data and seeking to keep the number of terms in the model low in the hopes that the terms that are given significant nonzero values through this procedure may be those with greatest physical relevance. For the purpose of modeling only, it is possible that neglecting terms on which a model only weakly depends may not significantly affect predictions of the process state; however, it is possible that some such terms have a physical meaning. To obtain a better understanding of a chemical process to enable factors affecting its economics and safety-based constraints to be accounted for in control design, it would be preferable to avoid the potential for neglecting physically relevant dependencies between states and inputs, even if they are weak. Another difficulty with using a method like that in Ref. [15] for a chemical process is that the nonlinearities present in chemical processes can be non-intuitive (e.g., one would be hard-pressed to guess the form of the rate law developed in Ref. [40] as a potential term for which coefficients should be identified in a model identification procedure). Furthermore, some coefficients which it may be desirable to determine from data for a chemical process (e.g., activation energies, powers in rate laws, coefficients of sums that appear in the denominator of a reaction rate law expression [41]), may appear nonlinearly, which can make linear regression techniques more difficult to apply to obtain these coefficients (though it is possible that there may be a way to rearrange the terms in the model to still identify them through a linear regression, as demonstrated in the section titled “Application to a Chemical Process Example” nonlinear optimization methods may not be ideal for identifying coefficients that appear nonlinearly because many nonlinear optimization algorithms locate local minima, and these would not be guaranteed to give physically meaningful values of parameters). The following numerical example illustrates the concepts just described.

Example 1. To exemplify the impacts of selecting inappropriate model structures on one’s ability to obtain a physically meaningful model, we consider an illustrative numerical example based on the following simple nonlinear system:

$$\dot{x} = ax^2 + bu \quad (30)$$

where x is the state of the system, u is an input, and $a, b \in \mathbb{R}$ are coefficients ($a = 0.35, b = 12.1$). The dynamic model in Eq 30 was integrated with an integration step of 10^{-3} time units, starting from the initial condition $x(t_0) = 6.3$ and with the following set of inputs $[-15, -5, -10, -10, -20, -2, -5, -10, -15]$, each component of which was held for 1,000 integration steps and stored every integration step to generate a data set. This set of manipulated inputs was chosen to maintain boundedness of x during the simulations performed. The model identification was performed using Ipopt [42] by minimizing the squared two-norm of the difference between the vector of measured values of x and the vector of the predictions of x (each prediction was determined by numerical integration from the measured value from 10^{-3} time units prior). The initial guess of each of the optimization variables in Ipopt was 10, the Ipopt tolerance was 10^{-7} , the limited memory Hessian approximation was selected, and the numerical approximations of the derivatives in the gradient of the objective function were performed with a centered finite difference approximation using a perturbation of 0.0001. When the terms for which the coefficients to be identified were only those on the right-hand side of Eq 30 (i.e., a and b were determined by the optimization problem), the solver returned approximately the correct values of the coefficients (specifically, $a = 0.350113$ and $b = 12.1007$). Another simulation

was performed in which the coefficients of four terms were determined such that the assumed dynamic model was as follows:

$$\dot{x} = \bar{a}x^2 + \bar{b}u + \bar{c}x + \bar{d}x^3 \quad (31)$$

In this case, the solution to the optimization problem was $\bar{a} = 0.347838$, $\bar{b} = 12.0996$, $\bar{c} = -0.00961972$, $\bar{d} = -8.11362 \times 10^{-5}$. The small values of \bar{c} and \bar{d} compared to the values of \bar{a} and \bar{b} suggest that the solver was able to determine a meaningful model (with respect to the actual process dynamics) when the terms for which coefficients were identified included those in the actual model, even when other terms were included as well. However, if no correct terms are selected for which the coefficients are determined, no meaningful model can be developed. For example, when the dynamic model was:

$$\dot{x} = \bar{e}x + \bar{f}u^2 + \bar{g}e^x + \bar{h}e^u \quad (32)$$

the coefficients identified by the optimization problem were $\bar{e} = -0.804014$, $\bar{f} = -0.109085$, $\bar{g} = 0.566903$, and $\bar{h} = 67.7681$. The resulting model is not meaningful with respect to the dynamics of the system.

DATA-GATHERING EMPC DESIGN

In this section, we suggest that controllers may help to address the challenges noted with respect to developing adequate structures for physically meaningful chemical process dynamic models and with respect to developing appropriate data for identification and validation of such models. Specifically, we present an EMPC design that is able to operate a chemical process in a nonroutine manner for short periods of time with the goal of manipulating the process state to achieve desired patterns in the process data that can be utilized to seek to obtain more physically meaningful process models from state measurements.

Data-Gathering EMPC Formulation

The proposed EMPC design is a modification of Eqs 18–22, where constraints can be added to the controller or terms can be added to the objective function that are multiplied by coefficients that can take either a zero or one value to represent that the modification is either off (not used to force the EMPC to gather the specific type of data implied by this constraint/term) or on (used by the EMPC to seek to obtain specific data). To clarify this concept, we present an example formulation of an EMPC that has the potential to move n_s selected components of the closed-loop state toward desired states $x_{d,i}$, $i = 1, \dots, n_s$, and n_k selected components of the manipulated input vector to desired values $u_{d,j}$, $j = 1, \dots, n_k$, while forcing changes in n_{ROC} selected components u_p , $p = 1, \dots, n_{ROC}$, of the input vector at each sampling time in the prediction horizon. This formulation is expressed by the following equations:

$$\begin{aligned} \min_{u(t) \in S(\Delta)} \int_{t_k}^{t_{k+N}} [L_c(\hat{x}(\tau), u(\tau)) + \delta_1 \sum_{j=1}^{n_k} \alpha_{w_j} (u_j(\tau) - u_{d,j})^2 + \delta_2 \sum_{i=1}^{n_s} \alpha_{y_i} (\hat{x}_i(\tau) - x_{d,i})^2 \\ - \delta_3 \sum_{q=k-1}^{k+N-2} \sum_{p=1}^{n_{ROC}} \alpha_{p,ROC} (u_p(t_q) - u_p(t_{q+1}))^2] d\tau \end{aligned} \quad (33)$$

$$\text{s.t. } \dot{\hat{x}} = f_{NL}(\hat{x}(t), u(t)) \quad (34)$$

$$\hat{x}(t_k) = x(t_k) \quad (35)$$

$$\hat{x}(t) \in X, \forall t \in [t_k, t_{k+N}) \quad (36)$$

$$u(t) \in U, \forall t \in [t_k, t_{k+N}) \quad (37)$$

$$g_{MPC}(\hat{x}, u) \leq 0 \quad (38)$$

where α_{wj} , for $j = 1, \dots, n_k$, α_{yi} , $i = 1, \dots, n_s$, and $\alpha_{p,ROC}$, for $p = 1, \dots, n_{ROC}$, are weighting constants, and $u_p(t_q)$, $p = 1, \dots, n_{ROC}$, represents the value of u_p computed for $t \in [t_q, t_{q+1})$ ($u_p(t_{k-1})$ represents the value of u_p applied for $t \in [t_{k-1}, t_k)$). The notation in Eqs 33–38 is like that in Eqs 18–22, but three additional terms have been added to the stage cost, which include penalties on the deviations of the selected components of the state and input vectors from desired values. The penalties in the objective function enforce desired “experimental” goals as soft constraints. The values of the terms δ_i , $i = 1, 2, 3$, depend on whether the terms in Eq 33 that each δ_i multiplies are selected to be activated ($\delta_i = 1$) or not ($\delta_i = 0$). The function g_{MPC} in Eq 38 represents any general inequality constraints in x and u that may be added to achieve online data-gathering goals; they may also include constraints added to maintain closed-loop stability. The model utilized for making state predictions in this MPC is the nonlinear empirical model of Eq 9, where \hat{x} represents predictions of the process state obtained from this empirical model. The empirical model is used because we assume that since we want to determine a physics-based model from data, we do not know the model of Eq 1.

Remark 2. If it is desired to obtain data where $u_j = u_{d,j}$, $j = 1, \dots, n_k$, or $\hat{x}_i = x_{d,i}$, $i = 1, \dots, n_s$, then it may be beneficial to make the weighting terms α_{wj} and α_{yi} large to attempt to drive these states to the desired values quickly (as deviation from the desired values will then make the objective function large) so that the online experiment can be completed relatively quickly and routine operation can be restored. Notably, once the states or inputs reach the desired values, the terms on the right-hand side of Eq 33 will be small, such that the economic objective function will become important (i.e., while data is being gathered with the states at their desired values, it will be gathered in the most economically optimal manner subject to values of some states being approximately constant; however, this may not be as economically optimal as the objective function without those states fixed, which is the motivation for seeking to complete the experiments quickly). Similarly, if $\delta_1 = \delta_2 = 0$, but $\delta_3 = 1$, though the penalty on the input rate of change is a negative addition to the objective function, this does not necessarily mean that the economics-based part of the stage cost is minimized more than if $\delta_3 = 0$ (the changes in the inputs encouraged by the input rate of change term in the objective function do not necessarily result in input trajectories that minimize L_e more than smaller input variations). It is therefore again desirable to seek to complete experiments quickly.

Remark 3. $u_{d,j}$ and $x_{d,i}$ are desired values that for the purposes of the formulation in Eq 33 are constant, though another EMPC formulation could be developed in which they change over time.

Data-Gathering EMPC Analysis

Several comments should be made with respect to the EMPC of Eqs 33–38 and EMPC's with similar on–off terms in the objective function and constraints to aid in gathering specific data for model identification (data-gathering EMPC's). First, the concept of obtaining “specific data” utilizing the proposed EMPC design should be clarified. In Eqs 33–38, the specific desired data is considered to be that which corresponds to the soft constraints being achieved (i.e., $u_j = u_{d,j}$ for $j = 1, \dots, n_k$, $x_i = x_{d,i}$ for $i = 1, \dots, n_s$, and significant changes between $u_p(t_q)$ and $u_p(t_{q+1})$ for $p = 1, \dots, n_{ROC}$, and $q = k - 1, \dots, k + N - 2$). Soft constraints are not guaranteed to be met, however, both because they may not be possible to achieve given the other constraints of the optimization problem (this would correspond to the case that they would be infeasible if they had been enforced as hard constraints) and because the minimum of the objective function does not necessarily correspond to all soft constraints being met (i.e., the terms in Eq 33 are competing with one another and with L_e when the EMPC is determining the values of u that most minimize the sum of all terms in Eq 33 given the constraints). However, Eqs 33–38 form only one example among many potential data-gathering EMPC formulations. Therefore, though the goal of these designs is to obtain specific data, there may be some formulations better suited to obtaining certain types of data than others for a given process, and some types of data may not be practically possible to obtain.

It can be expected that for the design of Eqs 33–38 to work well, sufficiently small errors are required between the actual and the empirical model so that sufficiently accurate process models are utilized to make predictions of the state when selecting input trajectories that optimize the objective function and meet the constraints. It would be expected that utilizing an empirical model that captures the physics of the process would allow the state predictions to be more accurate in a larger region of state-space, leading potentially to an increased ability of the EMPC to optimize profit [31,32] and, as would be important from a safety perspective, enabling the inputs it is computing to cause the system to more closely meet the constraints of the actual process if they caused these constraints to be met in the EMPC.

Without any conditions on the EMPC of Eqs 33–38, closed-loop stability of the process of Eq 1 operated under this EMPC and recursive feasibility of the EMPC optimization problem are not guaranteed. A variety of EMPC designs with a form similar to that in Eqs 33–38 at each sampling time have been developed with stability and feasibility guarantees in the case of no plant-model mismatch/disturbances (e.g., Refs. [43–46]). However, for the practical case considered in this article where the actual process dynamic model is unknown, it would be expected that there will be plant-model mismatch/disturbances, which motivates us to focus in a subsequent section on an example data-gathering EMPC formulation with guaranteed feasibility, stability, and robustness properties.

Another point with regard to data-gathering EMPC's is that the benefits of obtaining a physics-based model for EMPC can impact not only the state prediction accuracy but also the design of the controller. For example, unlike a tracking MPC, in which the form of the quadratic objective function is set *a priori* and the only adjustments made are in tuning the weighting matrices in the objective function, the objective function of EMPC is allowed to be a general profit measure. For some processes, profit may be a function of either a state or quantity that is not directly measured but is a function of other states that has significance because of its physical relevance with respect to the process dynamics (an example of this will be provided in the section titled “Application to a Chemical Process Example”).

In this case, obtaining a physics-based process model is key to being able to extract the relevant part of the dynamics that can be used to predict the process profit over time. Without such a means for obtaining the economic measure for an online process for which a first-principles model is not available, an economic measure that is not fully reflective of the process economics may be selected, which can lower the potential benefits of EMPC for such a process. Obtaining physics-based process models can also aid in developing important constraints for an EMPC design. It is sometimes desirable to constrain a combination of states, for example, and this combination may be dictated by the physics of the process but may not be readily discerned without a physical model. For example, in Ref. [47], a first-principles model for an ethylene oxidation process [48] coupled with a model for a valve experiencing stiction [49] is developed. Though the pressure applied to this valve by a pneumatic actuator is a function of the states and inputs (i.e., it was not itself a measured state), a constraint was imposed in the EMPC design on the pressure. In cases like this, it may be beneficial to develop physics-based dynamic models from which parts of the model which it is desired to constrain in the EMPC can be extracted for constraint design.

Remark 4. It is noted that the state predictions $\hat{x}(t)$ constitute a type of data for the system of Eq 9. In light of the concept that a data-gathering EMPC may be used to generate desired data from the system of Eq 1, it could also be explored whether it can generate desired data from the system of Eq 9. Specifically, MPC is implemented with a receding horizon and only the first input of the input trajectory that it computes at a given sampling time is applied to the process. Though it is beneficial to compute subsequent inputs in the prediction horizon to make the best possible selection of an input to apply from t_k to t_{k+1} based on longer-term profit and constraint satisfaction predictions (i.e., avoiding myopic behavior), it is possible to utilize the part of the prediction horizon after the first sampling period to, for short periods of time (to avoid possible degradation of profit or feasibility from these changes), perform “experiments” on the predicted state. In this case, it is possible to apply soft constraints as in the previous section but to have them activated only after the first sampling period to analyze the effects on the trajectory of the predicted states and to better understand their behavior.

Remark 5. It is conceivable that certain experiments may be preferably carried out in units with different designs than a unit has under routine operation (e.g., it is conceivable that certain types of data may be more readily generated in a continuous than a batch process, or vice versa). If it is believed that this may be the case, one could consider at the design stage of a process the types of data that it may be desirable to obtain online and the type of unit configuration necessary to achieve this and then develop the appropriate design/instrumentation (e.g., valves that are not typically actuated by a controller but can be opened or closed) at the key points in the process that would permit the desired unit configuration to be obtained for short periods of time for the purpose of gathering data. However, such a course of action has the potential to be complex (e.g., if a continuous process is switched to batch operation sometimes, some method for storing the fluid that would typically be flowing through the system would need to be developed to contain it during short-term batch operation) and must be rigorously investigated from a design, control, and control-theoretic perspective before being attempted. However, it is important to note that such manipulations may not be necessary. For example, in the section titled “Application to a Chemical Process Example”, a process example will be presented in

which creative manipulations of the process model with respect to regression techniques are used to derive reaction rate laws from operating data for a continuous process, though traditional chemical engineering design principles (e.g., Ref. [50]) suggest that batch experiments offer an effective reactor configuration for obtaining reaction rate data. This reflects that the controller and methods for getting models from data, when combined, may provide a good deal of power for obtaining information on the physics of the process.

Data-Gathering EMPC Implementation Strategy

An implementation strategy for data-gathering EMPC's should achieve the following goals:

- (1) determine how to initially operate a process for which the model, objective function, or constraints, or any combination thereof, may not be fully characterized because of a lack of complete knowledge of the process dynamics;
- (2) initiate desired experiments for short periods of time; and
- (3) update the model, objective function, and constraints of the EMPC once the experiments have improved the available information on the process dynamics.

To accomplish Goal 1, traditional methods for tracking MPC design with linear empirical models can be utilized because of their practical success in industry to date. Goal 2 can be pursued by developing a logic unit that determines the best times to turn on and off constraints ($\delta_i = 1$, or $\delta_i = 0$, $i = 1, 2, 3$, in Eq 33), either by receiving input from an engineer or through an automated method. The implementation strategy for a data-gathering EMPC design is as follows:

- Step 1.* Utilize standard industrial techniques for developing linear empirical models and MPC designs with quadratic objective functions for a process, develop an MPC design that uses a linear empirical model, and operate the process under this controller.
- Step 2.* Develop any additional terms in the objective function or constraints with their activation condition (e.g., δ) and set these terms/constraints to initially not be activated.
- Step 3.* When the logic unit indicates that one or more terms/constraints related to data-gathering should be activated, activate these terms/constraints at each sampling time to determine the MPC solution until the logic unit indicates that the constraint/term should be turned off. Repeat as necessary until it is determined that sufficient information has been obtained for attempting to identify a physics-based model.
- Step 4.* Process the obtained data to seek to develop a physics-based model.
- Step 5.* Analyze the obtained data to determine the types of data (not included in the training data) that would best verify the adequacy of the model to describe the process physics or determine what is still lacking.
- Step 6.* Perform the designated experiments according to *Step 5* by using the logic unit to indicate when constraints/terms should start and stop being used. If the predictions using the developed model match well with the nontraining data, continue to *Step 7*. If not, repeat *Steps 2–6*.
- Step 7.* Use the new dynamic model to update the constraints, objective function, and model in the MPC.
- Step 8.* Operate the process under this updated MPC until it is desired to reidentify a model to reduce plant–model mismatch or to change the objective function and constraints. When these changes become desired, repeat *Steps 2–8*.

Remark 6. It is likely that the modeling strategy described previously will need to be repeated over time. In particular, if a known persistent disturbance, fault, or process reconfiguration occurs, or sufficient time has elapsed since the last model identification such that slow changes in the process dynamics are to be expected to have occurred (because of, for

example, heat exchanger fouling or catalyst deactivation), this process may need to be re-executed.

EXAMPLE OF DATA-GATHERING EMPC WITH CLOSED-LOOP STABILITY GUARANTEES

In this section, we focus on an EMPC for which the constraint of Eq 38 takes a specific form as in Eqs 28 and 29 to provide guaranteed closed-loop stability, feasibility, and robustness properties.

Data-Gathering Lyapunov-Based EMPC Formulation

One may conceive of a large number of desired types of data that one may wish to obtain online using a data-gathering EMPC with Lyapunov-based stability constraints and, consequently, a large number of constraints or terms in the objective function that may be added in an effort to develop and validate a physics-based process model. We provide an example of an EMPC formulation that can handle several different types of experiments and demonstrates the flexibility of the control design for handling a variety of data-gathering objectives as follows:

$$\begin{aligned} \min_{u(t) \in S(\Delta)} \int_{t_k}^{t_{k+N}} [L_e(\hat{x}(\tau), u(\tau)) + \delta_1 \sum_{j=1}^{n_k} \alpha_{wj} (u_j(\tau) - u_{d,j})^2 + \delta_2 \sum_{i=1}^{n_s} \alpha_{yi} (\hat{x}_i(\tau) - x_{d,i})^2 \\ - \delta_3 \sum_{q=k-1}^{k+N-2} \sum_{p=1}^{n_{ROC}} \alpha_{p,ROC} (u_p(t_q) - u_p(t_{q+1}))^2] d\tau \end{aligned} \quad (39)$$

$$\text{s.t. } \dot{\hat{x}} = f_{NL}(\hat{x}(t), u(t)) \quad (40)$$

$$\hat{x}(t_k) = x(t_k) \quad (41)$$

$$\hat{x}(t) \in X, \forall t \in [t_k, t_{k+N}] \quad (42)$$

$$u(t) \in U, \forall t \in [t_k, t_{k+N}] \quad (43)$$

$$\hat{V}(\hat{x}(t)) \leq \hat{\rho}_e, \forall t \in [t_k, t_{k+N}] \quad \text{if } x(t_k) \in \Omega_{\hat{\rho}_e} \quad (44)$$

$$\begin{aligned} \frac{\partial \hat{V}(x(t_k))}{\partial x} (f_{NL}(x(t_k), u(t_k))) \\ \leq \frac{\partial \hat{V}(x(t_k))}{\partial x} (f_{NL}(x(t_k), h_{NL}(x(t_k)))) \quad \text{if } x(t_k) \notin \Omega_{\hat{\rho}_e} \\ \text{or } \delta_4 |x_i(t_k)| \geq \gamma_i, i = 1, \dots, n_f, \text{ or } t_k \geq t', \text{ or } \delta_5 = 1 \end{aligned} \quad (45)$$

where the notation follows that of Eqs 33–38 except that the constraint of Eq 38 is replaced by the Lyapunov-based stability constraints of Eqs 44 and 45. This is a form of LEMPC using an empirical process model [31,32]. In addition to δ_1 , δ_2 , and δ_3 , which have the same purpose as they do in Eqs 33–38, δ_4 , and δ_5 are also parameters in this equation that take a value of either zero or one, depending on whether it is desired to utilize the constraint of Eq 45 that they activate or not. Specifically, when $\delta_4 = \delta_5 = 0$ and $t_k < t'$, the LEMPC seeks to maintain the predictions of the closed-loop state obtained from the empirical model of Eq 40 in the level set $\Omega_{\hat{\rho}_e}$ of \hat{V} . When the closed-loop state exits this region, the constraint of Eq 45 is activated to drive the closed-loop state back into $\Omega_{\hat{\rho}_e}$. t' is a predetermined time after which it is desired to enforce the constraint of Eq 45 in the

LEMPC regardless of whether $x(t_k) \in \Omega_{\hat{\rho}_e}$ or not, with the goal of driving the closed-loop state to a neighborhood of the origin in finite time. If $t_k < t'$, then when $\delta_5 = 1$, Eq 45 is again activated repeatedly regardless of whether $x(t_k) \in \Omega_{\hat{\rho}_e}$ or not to drive the closed-loop state toward a neighborhood of the origin. The difference between setting $\delta_5 = 1$ and having $t_k \geq t'$ is that it is assumed that after t' , the constraint of Eq 45 is not again inactivated, whereas it is not necessary to maintain $\delta_5 = 1$ for all times, such that the constraint of Eq 45 can be activated for finite periods of time when $x(t_k) \in \Omega_{\hat{\rho}_e}$ by this condition. The term containing δ_4 is also used to activate Eq 45 regardless of the location of $x(t_k)$ in state-space, but unlike δ_5 , it is used to activate Eq 45 only when the magnitudes of the n_f components of the measured state vector are not within the corresponding γ_i of their steady-state value [51]. Because the γ_i , $i = 1, \dots, n_f$, are taken to be positive constants, when $\delta_4 = 0$, then $\delta_4|x_i(t_k)| = 0$ cannot be greater than or equal to γ_i , which means that the condition $\delta_4|x_i(t_k)| \geq \gamma_i$ cannot be used to activate Eq 45. However, if $\delta_4 = 1$, then whenever the measured values of any of the n_f states x_i at t_k are more than γ_i from their steady-state values, Eq 45 is activated to attempt to drive the closed-loop state of Eq 1 closer to its steady-state value. The γ_i may be chosen based on the amount of deviation of x_i , $i = 1, \dots, n_f$, that an engineer would like to allow for each x_i , $i = 1, \dots, n_f$, from its steady-state value; however, as will be demonstrated in the section titled “Data-Gathering LEMPC Stability Analysis,” the closed-loop state is only guaranteed to be able to be driven into a region where $|x_i(t_k)| < \gamma_i$, $i = 1, \dots, n_f$, if certain conditions are met on γ_i . The implementation strategy for the LEMPC of Eqs 39–45 is like that for the EMPC of Eqs 33–38 that is outlined in the section titled “Data-Gathering EMPC Implementation Strategy,” except that provision must be made for developing the Lyapunov-based stability constraints whenever the model updates, and furthermore, the model updates must take place in a manner that maintains closed-loop stability and recursive feasibility. Specifically, the modifications to the implementation strategy in the section titled “Data-Gathering EMPC Implementation Strategy” are that in *Step 1*, the design of the LEMPC should include appropriate design of $\hat{\rho}$, $\hat{\rho}_e$, \hat{V} , and h_{NL} . Furthermore, in *Step 7*, these parameters should be updated as necessary for the new model, and it should be ensured that before the model is updated, the closed-loop state is driven into a region where the model can be changed with closed-loop stability and feasibility guarantees (this region can be a region of overlap between the stability regions associated with the new and old models, which will be clarified in the section titled “Data-Gathering LEMPC Stability Analysis”).

Data-Gathering LEMPC Stability Analysis

In this section, we prove recursive feasibility and closed-loop stability of the process of Eq 1 under the LEMPC of Eqs 39–45. We first present three propositions used in the proofs of the three theorems to be presented.

Proposition 1. [32] *Consider the systems*

$$\dot{x}_a = f(x_a(t), u(t), w(t)) \quad (46)$$

$$\dot{x}_b = f_{NL}(x_b(t), u(t)) \quad (47)$$

with initial states $x_a(t_0) = x_b(t_0) \in \Omega_{\hat{\rho}}$ with $t_0 = 0$, $u \in U$, and $w \in W$. If $x_a(t), x_b(t) \in \Omega_{\hat{\rho}}$ for $t \in [0, T]$ then there exists a function $f_W(\cdot)$ such that

$$|x_a(t) - x_b(t)| \leq f_w(t) \quad (48)$$

with

$$f_w(t) := \frac{\bar{L}_w \Theta + M_{err}}{\bar{L}_x} (e^{\bar{L}_x t} - 1) \quad (49)$$

where M_{err} is defined by the following:

$$|f(x, u, 0) - f_{NL}(x, u)| \leq M_{err}, \forall x \in \Omega_\rho \text{ and } u \in U. \quad (50)$$

Proof. From the statement of Proposition 1, $x_a(0) = x_b(0) = x_0$. From Eqs 46 and 47, we obtain the following:

$$\begin{aligned} x_a(t) &= x_0 + \int_0^t f(x_a(s), u(s), w(s)) ds \\ x_b(t) &= x_0 + \int_0^t f_{NL}(x_b(s), u(s)) ds \end{aligned} \quad (51)$$

Then,

$$\begin{aligned} x_a(t) - x_b(t) &= \int_0^t [f(x_a(s), u(s), w(s)) - f_{NL}(x_b(s), u(s))] ds \\ |x_a(t) - x_b(t)| &= \left| \int_0^t [f(x_a(s), u(s), w(s)) - f_{NL}(x_b(s), u(s))] ds \right| \\ &\leq \int_0^t |f(x_a(s), u(s), w(s)) - f_{NL}(x_b(s), u(s))| ds \\ &= \int_0^t |f(x_a(s), u(s), w(s)) - f(x_b(s), u(s), 0) \\ &\quad + f(x_b(s), u(s), 0) - f_{NL}(x_b(s), u(s))| ds \end{aligned} \quad (52)$$

From Eq 16, which holds in the region Ω_ρ under consideration, we obtain the following:

$$\begin{aligned} |x_a(t) - x_b(t)| &\leq \int_0^t [\bar{L}_x |x_a(s) - x_b(s)| + \bar{L}_w |w(s)| \\ &\quad + |f(x_b(s), u(s), 0) - f_{NL}(x_b(s), u(s))|] ds \end{aligned} \quad (53)$$

for all times between $t_0 = 0$ and t . Because $|w(t)| \leq \Theta$, the last inequality can be written as follows:

$$\begin{aligned} |x_a(t) - x_b(t)| &\leq \int_0^t [\bar{L}_x |x_a(s) - x_b(s)| + \bar{L}_w \Theta \\ &\quad + |f(x_b(s), u(s), 0) - f_{NL}(x_b(s), u(s))|] ds \end{aligned} \quad (54)$$

From the definition of $M_{err} > 0$ in Eq 50, we obtain

$$|x_a(t) - x_b(t)| \leq \int_0^t [\bar{L}_x |x_a(s) - x_b(s)| + \bar{L}_w \Theta + M_{err}] ds \quad (55)$$

$$\leq (\bar{L}_w \Theta + M_{err})t + \int_0^t [\bar{L}_x |x_a(s) - x_b(s)|] ds \quad (56)$$

for times between $t_0 = 0$ and t . From the Gronwall-Bellman inequality [52], we obtain the following:

$$|x_a(t) - x_b(t)| \leq \frac{\bar{L}_w \Theta + M_{err}}{\bar{L}_x} (e^{\bar{L}_x t} - 1) \quad (57)$$

Proposition 2. [53] Consider the Lyapunov function $\hat{V}(\cdot)$ of the nominal system of Eq 9 under the controller $h_{NL}(x)$ that meets Eqs 10–13. There exists a quadratic function $f_V(\cdot)$ such that

$$\hat{V}(x) \leq \hat{V}(\bar{x}) + f_V(|x - \bar{x}|) \quad (58)$$

for all $x, \bar{x} \in \Omega_{\hat{\rho}}$ with

$$f_V(s) := \hat{\alpha}_4(\hat{\alpha}_1^{-1}(\hat{\rho}))s + M_v s^2 \quad (59)$$

where M_v is a positive constant.

Proposition 3. Consider the closed-loop system of Eq 9 under $h_{NL}(\hat{x})$ that satisfies the inequalities of Eqs 10–13 in sample-and-hold. Let $\Delta > 0$, $\hat{e}_W > 0$, and $\hat{\rho} > \hat{\rho}_e > \hat{\rho}_{\min} > \hat{\rho}_s > 0$ satisfy

$$-\hat{\alpha}_3(\hat{\alpha}_2^{-1}(\hat{\rho}_s)) + L_L M_L \Delta \leq -\hat{e}_W / \Delta \quad (60)$$

and

$$\hat{\rho}_{\min} := \max\{\hat{V}(\hat{x}(t + \Delta)) : \hat{V}(\hat{x}(t)) \leq \hat{\rho}_s\}. \quad (61)$$

If $\hat{x}(0) \in \Omega_{\hat{\rho}}$, then:

$$\hat{V}(\hat{x}(t_{k+1})) - \hat{V}(\hat{x}(t_k)) \leq -\hat{e}_W \quad (62)$$

for $\hat{x}(t_k) \in \Omega_{\hat{\rho}} / \Omega_{\hat{\rho}_s}$ and the state trajectory $\hat{x}(t)$ of the closed-loop system is always bounded in $\Omega_{\hat{\rho}}$ for $t \geq 0$ and is ultimately bounded in $\Omega_{\hat{\rho}_{\min}}$.

Proof. We obtain from Eq 11 that

$$\frac{\partial \hat{V}(\hat{x}(t_k))}{\partial \hat{x}} (f_{NL}(\hat{x}(t_k), h_{NL}(\hat{x}(t_k)))) \leq -\hat{\alpha}_3(|\hat{x}(t_k)|) \quad (63)$$

For $t \in [t_k, t_{k+1})$, the following inequalities are obtained:

$$\begin{aligned} & \frac{\partial \hat{V}(\hat{x}(t))}{\partial \hat{x}} (f_{NL}(\hat{x}(t), h_{NL}(\hat{x}(t_k)))) \\ &= \frac{\partial \hat{V}(\hat{x}(t))}{\partial \hat{x}} (f_{NL}(\hat{x}(t), h_{NL}(\hat{x}(t_k)))) \\ &+ \frac{\partial \hat{V}(\hat{x}(t_k))}{\partial \hat{x}} (f_{NL}(\hat{x}(t_k), h_{NL}(\hat{x}(t_k)))) \\ &- \frac{\partial \hat{V}(\hat{x}(t_k))}{\partial \hat{x}} (f_{NL}(\hat{x}(t_k), h_{NL}(\hat{x}(t_k)))) \\ &\leq -\hat{\alpha}_3(|\hat{x}(t_k)|) + L_L |\hat{x}(t) - \hat{x}(t_k)| \end{aligned} \quad (64)$$

where the last inequality follows from Eqs 63 and 15. For $t \in [t_k, t_{k+1})$, the continuity of \hat{x} and Eq 14 lead to the following bound:

$$|\hat{x}(t) - \hat{x}(t_k)| \leq M_L \Delta \quad (65)$$

From Eqs 64 and 65, we obtain the following bound on the time derivative of the Lyapunov function:

$$\frac{\partial \hat{V}(\hat{x}(t))}{\partial \hat{x}} (f_{NL}(\hat{x}(t), h_{NL}(\hat{x}(t_k)))) \leq -\hat{\alpha}_3(|\hat{x}(t_k)|) + L_L M_L \Delta \quad (66)$$

for $t \in [t_k, t_{k+1})$. When $\hat{x}(t_k) \in \Omega_{\hat{\rho}}/\Omega_{\hat{\rho}_s}$, then from Eq 10, $\hat{\rho}_s \leq \hat{\alpha}_2(|\hat{x}(t_k)|)$, which gives the following:

$$\frac{\partial \hat{V}(\hat{x}(t))}{\partial \hat{x}} (f_{NL}(\hat{x}(t), h_{NL}(\hat{x}(t_k)))) \leq -\hat{\alpha}_3(\hat{\alpha}_2^{-1}(\hat{\rho}_s)) + L_L M_L \Delta \quad (67)$$

for $t \in [t_k, t_{k+1})$. If Eq 60 is satisfied, then

$$\frac{\partial \hat{V}(\hat{x}(t))}{\partial \hat{x}} (f_{NL}(\hat{x}(t), h_{NL}(\hat{x}(t_k)))) \leq -\hat{e}_W/\Delta \quad (68)$$

for $t \in [t_k, t_{k+1})$. Integrating the bound in Eq 68 for $t \in [t_k, t_{k+1})$ gives the following:

$$\hat{V}(\hat{x}(t_{k+1})) \leq \hat{V}(\hat{x}(t_k)) - \hat{e}_W, \quad (69)$$

$$\hat{V}(\hat{x}(t)) \leq \hat{V}(\hat{x}(t_k)), \forall t \in [t_k, t_{k+1}] \quad (70)$$

when $\hat{x}(t_k) \in \Omega_{\hat{\rho}}/\Omega_{\hat{\rho}_s}$. When $\hat{x}(t_k) \in \Omega_{\hat{\rho}_s}$, then from Eq 61, $\hat{x}(t_{k+1}) \in \Omega_{\hat{\rho}_{\min}}$. Therefore, when the empirical system of Eq 9 is controlled using $h_{NL}(x)$ in sample-and-hold, the Lyapunov function will decrease for each sampling time until the closed-loop state reaches $\Omega_{\hat{\rho}_{\min}}$, within which it will remain thereafter.

It is noted that Eq 61 defines $\hat{\rho}_{\min}$ as the largest possible value of \hat{V} within one sampling period if $\hat{x}(t_k) \in \Omega_{\hat{\rho}_s}$, for any $u \in U$. The conditions under which the closed-loop state of Eq 1 under the LEMPC of Eqs 39–45 is bounded in $\Omega_{\hat{\rho}}$ and ultimately bounded in $\Omega_{\hat{\rho}_{\min}}$ are next presented.

Theorem 1. Consider the closed-loop system of Eq 1 under the LEMPC of Eqs 39–45 based on the controller $h_{NL}(x)$ that satisfies the inequalities in Eqs 10–13. Let $\epsilon_W > 0$, $\Delta > 0$, $N \geq 1$, and $\hat{\rho} > \hat{\rho}_e > \hat{\rho}_{\min} > \hat{\rho}_s > 0$ satisfy:

$$-\hat{\alpha}_3(\hat{\alpha}_2^{-1}(\hat{\rho}_e)) + \hat{\alpha}_4(\hat{\alpha}_1^{-1}(\hat{\rho}))M_{err} + \bar{L}'_x M \Delta + \bar{L}'_w \Theta \leq -\epsilon_W/\Delta \quad (71)$$

$$\hat{\rho}_e \leq \hat{\rho} - f_V(f_W(\Delta)) \quad (72)$$

If $x(0) \in \Omega_{\hat{\rho}}$, and Proposition 3 is satisfied, then the state trajectory $x(t)$ of the closed-loop system is always bounded in $\Omega_{\hat{\rho}}$ for $t \geq 0$. Furthermore, if $t > t'$ and

$$-\hat{\alpha}_3(\hat{\alpha}_2^{-1}(\hat{\rho}_s)) + \hat{\alpha}_4(\hat{\alpha}_1^{-1}(\hat{\rho}))M_{err} + \bar{L}'_x M \Delta + \bar{L}'_w \Theta \leq -\epsilon_W/\Delta \quad (73)$$

then the state trajectory $x(t)$ of the closed-loop system is ultimately bounded in $\Omega_{\hat{\rho}_{\min}}$.

Proof. The proof is divided into two parts. In the first part, the feasibility of the LEMPC optimization problem will be discussed when the state is maintained in $\Omega_{\hat{\rho}}$. Then, in the

second part, it will be proven that the closed-loop state under the LEMPC of Eqs 39–45 is always bounded in $\Omega_{\hat{\rho}}$ and is ultimately bounded in $\Omega_{\hat{\rho}_{\min}}$.

Part 1. From Proposition 3, the controller h_{NL} in sample-and-hold can maintain the closed-loop state of the system of Eq 40 within $\Omega_{\hat{\rho}}$. Because $\Omega_{\hat{\rho}}$ has been defined as a region within which the state constraints are met, Eq 42 is therefore met under h_{NL} in sample-and-hold. The input constraint (Eq 43) is also feasible because $h_{NL}(x) \in U$ from Eq 13. Furthermore, from Proposition 3, $h_{NL}(\hat{x}(t_q))$, $q = k, \dots, k + N - 1$, $t \in [t_q, t_{q+1})$, maintains the closed-loop state in $\Omega_{\hat{\rho}_e}$ when $x(t_k) \in \Omega_{\hat{\rho}_e}$ for $\hat{\rho}_e > \hat{\rho}_{\min}$ because it does not allow the Lyapunov function to increase until $x(t) \in \Omega_{\hat{\rho}_s}$ and then it maintains the closed-loop state in $\Omega_{\hat{\rho}_{\min}}$. Therefore, h_{NL} in sample-and-hold satisfies the constraint of Eq 44. Finally, Eq 45 is trivially satisfied by $h_{NL}(\hat{x}(t_k))$, such that h_{NL} in sample-and-hold also ensures feasibility of this constraint. Feasibility of each constraint of Eqs 39–45 is thus established at every sampling time under h_{NL} in sample-and-hold, regardless of the values of δ_i , $i = 1, 2, 3, 4, 5$.

Part 2. We now prove that if $x(t_0) \in \Omega_{\hat{\rho}}$, $x(t) \in \Omega_{\hat{\rho}}$, $\forall t \geq 0$. We proceed by developing results on the trajectory $x(t)$, $t \in [t_k, t_{k+1})$, given $x(t_k) \in \Omega_{\hat{\rho}}$, and assuming $\delta_4 = \delta_5 = 0$. We then extend the results to the case that $x(t_0) \in \Omega_{\hat{\rho}}$ and δ_4 or δ_5 or both can be 1 for some samplings periods.

If $x(t_0) \in \Omega_{\hat{\rho}}/\Omega_{\hat{\rho}_e}$ and $\delta_4 = \delta_5 = 0$, then

$$\begin{aligned} & \frac{\partial \hat{V}(x(t_k))}{\partial x} (f_{NL}(x(t_k), u(t_k))) \\ & \leq \frac{\partial \hat{V}(x(t_k))}{\partial x} (f_{NL}(x(t_k), h_{NL}(x(t_k)))) \leq -\hat{\alpha}_3(|x(t_k)|) \end{aligned} \quad (74)$$

which follows from Eqs 45 and 11. A bound on the time derivative of the Lyapunov function at t_k along the closed-loop state trajectory of the nominal system of Eq 1 under $h_{NL}(x(t_k))$ can also be developed as follows:

$$\begin{aligned} & \frac{\partial \hat{V}(x(t_k))}{\partial x} (f(x(t_k), h_{NL}(x(t_k)), 0)) \\ & = \frac{\partial \hat{V}(x(t_k))}{\partial x} (f_{NL}(x(t_k), h_{NL}(x(t_k)))) \\ & + \frac{\partial \hat{V}(x(t_k))}{\partial x} (f(x(t_k), h_{NL}(x(t_k)), 0)) \\ & - \frac{\partial \hat{V}(x(t_k))}{\partial x} (f_{NL}(x(t_k), h_{NL}(x(t_k)))) \\ & \leq -\hat{\alpha}_3(|x(t_k)|) + \left| \frac{\partial \hat{V}(x(t_k))}{\partial x} \right| |f(x(t_k), h_{NL}(x(t_k)), 0) \\ & - f_{NL}(x(t_k), h_{NL}(x(t_k)))| \end{aligned} \quad (75)$$

$\forall x(t_k) \in D_{NL}$. Applying the definition of M_{err} in Eqs 50 and 12 to Eq 75, we obtain the following:

$$\frac{\partial \hat{V}(x(t_k))}{\partial x} (f(x(t_k), h_{NL}(x(t_k)), 0)) \leq -\hat{\alpha}_3(|x(t_k)|) + \hat{\alpha}_4(|x(t_k)|) M_{err} \quad (76)$$

for any $x(t_k) \in \Omega_{\hat{\rho}}$. The time derivative of the Lyapunov function along the state

trajectory of the closed-loop nonlinear system of Eq 1 under h_{NL} implemented in sample-and-hold is

$$\begin{aligned}
& \frac{\partial \hat{V}(x(\tau))}{\partial x}(f(x(\tau), h_{NL}(x(t_k)), w(\tau))) \\
&= \frac{\partial \hat{V}(x(\tau))}{\partial x}(f(x(\tau), h_{NL}(x(t_k)), w(\tau))) \\
&\quad - \frac{\partial \hat{V}(x(t_k))}{\partial x}(f(x(t_k), h_{NL}(x(t_k)), 0)) \\
&\quad + \frac{\partial \hat{V}(x(t_k))}{\partial x}(f(x(t_k), h_{NL}(x(t_k)), 0)) \\
&\leq \left| \frac{\partial \hat{V}(x(\tau))}{\partial x}(f(x(\tau), h_{NL}(x(t_k)), w(\tau))) \right. \\
&\quad \left. - \frac{\partial \hat{V}(x(t_k))}{\partial x}(f(x(t_k), h_{NL}(x(t_k)), 0)) \right| \\
&\quad - \hat{\alpha}_3(|x(t_k)|) + \hat{\alpha}_4(|x(t_k)|)M_{err}
\end{aligned} \tag{77}$$

for $\tau \in [t_k, t_{k+1})$, where the last inequality follows from Eq 76 and the triangle inequality. From Eq 17, Eqs 10–12, the bound on w , Eq 8 and the continuity of x , and considering that $x(t_k) \in \Omega_{\hat{\rho}}/\Omega_{\hat{\rho}_e}$, we obtain from Eq 77 that for $\tau \in [t_k, t_{k+1})$

$$\frac{\partial \hat{V}(x(\tau))}{\partial x}(f(x(\tau), h_{NL}(x(t_k)), w(\tau))) \tag{78}$$

$$\leq \bar{L}'_x|x(\tau) - x(t_k)| + \bar{L}'_w|w| - \hat{\alpha}_3(|x(t_k)|) + \hat{\alpha}_4(|x(t_k)|)M_{err} \tag{79}$$

$$\leq \bar{L}'_x M \Delta + \bar{L}'_w \Theta - \hat{\alpha}_3(\hat{\alpha}_2^{-1}(\hat{\rho}_e)) + \hat{\alpha}_4(\hat{\alpha}_1^{-1}(\hat{\rho}))M_{err} \tag{80}$$

We seek an upper bound on $\dot{\hat{V}}$ along the closed-loop state trajectories of the system of Eq 1 under $u(t_k)$ computed by the LEMPC of Eqs 39–45 and applied for $t \in [t_k, t_{k+1})$. We first obtain an expression for $\dot{\hat{V}}$ in this case if $w(t) \equiv 0$. Following similar steps as in Eq 75, we obtain

$$\begin{aligned}
& \frac{\partial \hat{V}(x(t_k))}{\partial x}(f(x(t_k), u(t_k), 0)) \\
&= \frac{\partial \hat{V}(x(t_k))}{\partial x}(f_{NL}(x(t_k), u(t_k))) \\
&\quad + \frac{\partial \hat{V}(x(t_k))}{\partial x}(f(x(t_k), u(t_k), 0)) \\
&\quad - \frac{\partial \hat{V}(x(t_k))}{\partial x}(f_{NL}(x(t_k), u(t_k))) \\
&\leq -\hat{\alpha}_3(|x(t_k)|) + \left| \frac{\partial \hat{V}(x(t_k))}{\partial x}(f(x(t_k), u(t_k), 0)) \right. \\
&\quad \left. - \frac{\partial \hat{V}(x(t_k))}{\partial x}(f_{NL}(x(t_k), u(t_k))) \right|
\end{aligned} \tag{81}$$

where the last inequality follows from Eq 74 and the triangle inequality. Using similar steps as in Eqs 75 and 76, we obtain the following:

$$\frac{\partial \hat{V}(x(t_k))}{\partial x}(f(x(t_k), u(t_k), 0)) \leq -\hat{\alpha}_3(|x(t_k)|) + \hat{\alpha}_4(|x(t_k)|)M_{err} \quad (82)$$

This inequality can be used in the following with similar steps as were taken to arrive at Eq 80:

$$\begin{aligned} & \frac{\partial \hat{V}(x(\tau))}{\partial x}(f(x(\tau), u(t_k), w(\tau))) \\ &= \frac{\partial \hat{V}(x(\tau))}{\partial x}(f(x(\tau), u(t_k), w(\tau))) \\ &+ \frac{\partial \hat{V}(x(t_k))}{\partial x}(f(x(t_k), u(t_k), 0)) \\ &- \frac{\partial \hat{V}(x(t_k))}{\partial x}(f(x(t_k), u(t_k), 0)) \\ &\leq -\hat{\alpha}_3(|x(t_k)|) + \hat{\alpha}_4(|x(t_k)|)M_{err} \\ &+ \left| \frac{\partial \hat{V}(x(\tau))}{\partial x}(f(x(\tau), u(t_k), w(\tau))) \right. \\ &\quad \left. - \frac{\partial \hat{V}(x(t_k))}{\partial x}(f(x(t_k), u(t_k), 0)) \right| \\ &\leq -\hat{\alpha}_3(\hat{\alpha}_2^{-1}(\hat{\rho}_e)) + \hat{\alpha}_4(\hat{\alpha}_1^{-1}(\hat{\rho}))M_{err} + \bar{L}'_x M \Delta + \bar{L}'_w \Theta \end{aligned} \quad (83)$$

for $\tau \in [t_k, t_{k+1})$. From Eqs 83 and 71, the following statement holds:

$$\begin{aligned} \hat{V}(x(t_{k+1})) - \hat{V}(x(t_k)) &\leq -\epsilon_W \\ \hat{V}(x(\tau)) &\leq \hat{V}(x(t_k)), \forall \tau \in [t_k, t_{k+1}] \end{aligned} \quad (84)$$

when $x(t_k) \in \Omega_{\hat{\rho}}/\Omega_{\hat{\rho}_e}$, and the Lyapunov function value will decrease over a sampling period, and $x(t) \in \Omega_{\hat{\rho}}$, $\forall t \in [t_k, t_{k+1}]$. This indicates that if the constraint of Eq 45 is applied for consecutive sampling periods, then in a finite number of sampling periods, $x(t)$ will re-enter the region $\Omega_{\hat{\rho}_e}$.

When $x(t_k) \in \Omega_{\hat{\rho}_e}$ and $\delta_4 = \delta_5 = 0$, then, assuming that $x(t) \in \Omega_{\hat{\rho}}$ for $t \in [t_k, t_{k+1})$, the following holds from Propositions 1 and 2 and Eq 44:

$$\begin{aligned} \hat{V}(x(t)) &\leq \hat{V}(\hat{x}(t)) + f_V(|x(t) - \hat{x}(t)|) \\ &\leq \hat{\rho}_e + f_V(f_W(\Delta)) \end{aligned} \quad (85)$$

for $t \in [t_k, t_{k+1})$. If Eq 72 holds, $\hat{V}(x(t)) \leq \hat{\rho}$ for $t \in [t_k, t_{k+1})$ and therefore when $x(t_k) \in \Omega_{\hat{\rho}_e}$, $x(t) \in \Omega_{\hat{\rho}}$ for $t \in [t_k, t_{k+1})$ as assumed.

We now prove ultimate boundedness of the state trajectories in $\Omega_{\hat{\rho}_{\min}}$. In Eqs 74–84, it was proven that when $x(t_k) \in \Omega_{\hat{\rho}}/\Omega_{\hat{\rho}_e}$ such that the constraint of Eq 45 holds, then $\hat{V}(x(t_{k+1})) < \hat{V}(x(t_k))$. When $t_k \geq t'$ and $\delta_4 = \delta_5 = 0$, Eq 45 holds even if $x(t_k) \in \Omega_{\hat{\rho}_e}$. Therefore, using a similar series of steps as in Eqs 74–84 but considering $x(t_k) \in \Omega_{\hat{\rho}}/\Omega_{\hat{\rho}_s}$, and with Eq 73, we obtain that Eq 84 holds for all $x(t_k) \in \Omega_{\hat{\rho}}/\Omega_{\hat{\rho}_s}$, indicating that when $t_k \geq t'$ and $\delta_4 = \delta_5 = 0$, the closed-loop state is driven into $\Omega_{\hat{\rho}_s} \subset \Omega_{\hat{\rho}_{\min}}$ in finite time. Once the closed-loop state enters $\Omega_{\hat{\rho}_{\min}}$, then from the definition of $\Omega_{\hat{\rho}_{\min}}$ in

Eq 61, the closed-loop state remains in $\Omega_{\hat{\rho}_{\min}}$ because if $x(t_k) \in \Omega_{\hat{\rho}_s}$, then $x(t_{k+1}) \in \Omega_{\hat{\rho}_{\min}}$, and if $x(t_k) \in \Omega_{\hat{\rho}_{\min}}/\Omega_{\hat{\rho}_s}$, then $V(x(t_{k+1})) < V(x(t_k))$, and therefore $x(t_{k+1}) \in \Omega_{\hat{\rho}_{\min}}$.

To complete the proof, we first note that whether $x(t_k) \in \Omega_{\hat{\rho}}/\Omega_{\hat{\rho}_e}$, $x(t_k) \in \Omega_{\hat{\rho}_e}$, or $x(t_k) \in \Omega_{\hat{\rho}_{\min}}$, it was demonstrated that $x(t) \in \Omega_{\hat{\rho}}$ for $t \in [t_k, t_{k+1})$. This indicates that if $x(t_0) \in \Omega_{\hat{\rho}}$, the closed-loop state cannot leave $\Omega_{\hat{\rho}}$ within any subsequent sampling period, and therefore $x(t) \in \Omega_{\hat{\rho}}$ for all $t \geq 0$, if $\delta_4 = \delta_5 = 0$.

Finally, we note that the results of Eq 84 when $x(t_k) \in \Omega_{\hat{\rho}}/\Omega_{\hat{\rho}_s}$ depend only on activation of the constraint of Eq 45. Therefore, if δ_4 or δ_5 is 1, which causes Eq 45 to hold regardless of whether $x(t_k) \in \Omega_{\hat{\rho}_e}$, their effect is to cause Eq 84 to hold if $x(t_k) \in \Omega_{\hat{\rho}}/\Omega_{\hat{\rho}_s}$ or Eq 61 if $x(t_k) \in \Omega_{\hat{\rho}_s}$. It was proven previously that when Eqs 84 and 61 hold at a sampling time and the conditions of Theorem 1 are met, $x(t) \in \Omega_{\hat{\rho}}$ for $t \in [t_k, t_{k+1})$. Furthermore, the proof of closed-loop stability was independent of the objective function value of Eq 40, and therefore is unaffected by the values of δ_1 , δ_2 , or δ_3 . Therefore, whether the δ_i , $i = 1, 2, 3, 4, 5$, are 1 or 0, $x(t) \in \Omega_{\hat{\rho}}$, for all $t \geq 0$, if $x(t_0) \in \Omega_{\hat{\rho}}$.

The following theorem presents the conditions that guarantee the LEMPC formulation of Eqs 39–45 is able to drive the closed-loop state to either a region where $|x_i(t_k)| < \gamma_i$, $i = 1, \dots, n_f$ or to $\Omega_{\hat{\rho}_{\min}}$ when driving the closed-loop state to one of these regions becomes desirable for the purposes of achieving the goals of an online experiment.

Theorem 2. Consider the closed-loop system of Eq 1 under the LEMPC of Eqs 39–45, and consider that the conditions of Theorem 1 hold. If $\delta_5 = 1$ for at least $\lfloor \frac{t_h}{\Delta} + 1 \rfloor$ consecutive sampling periods, where $t_h = -\frac{\Delta(\hat{\rho}_{\min} - \hat{\rho})}{\epsilon_w}$, then it is guaranteed that the closed-loop state is driven into $\Omega_{\hat{\rho}_{\min}}$ within t_h time units for any $x(t_k) \in \Omega_{\hat{\rho}}$. Furthermore, if $\Omega_{\hat{\rho}_{\min}}$ is contained in the region where $|x_i(t_k)| < \gamma_i$, $i = 1, \dots, n_f$, then the state trajectory $x(t)$ is guaranteed to be driven into the region where $|x_i(t_k)| < \gamma_i$, $i = 1, \dots, n_f$, within t_h time units if $\delta_4 = 1$ for at least $\lfloor \frac{t_h}{\Delta} + 1 \rfloor$ consecutive sampling periods.

Proof. The proof for this theorem is divided into two parts: the first will prove the result for $\delta_5 = 1$, and the other will prove the result for $\delta_4 = 1$.

Part 1. When $\delta_5 = 1$, the constraint of Eq 45 is activated, and Eq 83 holds, meaning:

$$\frac{\partial \hat{V}(x(\tau))}{\partial x} f(x(\tau), u(t_k), w(\tau)) \leq -\epsilon_w / \Delta \quad (86)$$

holds for $\tau \in [t_k, t_{k+1})$, for any $x(t_k) \in \Omega_{\hat{\rho}}/\Omega_{\hat{\rho}_s}$ because the conditions of Theorem 1 are assumed to be satisfied. To develop a worst-case value of t_h , consider that $x(t_k)$ is as far from $\Omega_{\hat{\rho}_{\min}}$ as possible within $\Omega_{\hat{\rho}}$ (i.e., $V(x(t_k)) = \hat{\rho}$). Then the integral of Eq 86 considering $\hat{V}(x(t_k)) = \hat{\rho}$ and $\hat{V}(x(t_k + t_h)) = \hat{\rho}_{\min}$ gives $t_h = -\Delta(\hat{\rho}_{\min} - \hat{\rho})/\epsilon_w$. Because t_h is not guaranteed to be an integer multiple of a sampling period, the constraint of Eq 45 must be activated for $\lfloor \frac{t_h}{\Delta} + 1 \rfloor$ sampling periods to ensure that it is activated for no less than the amount of time required for the closed-loop state to enter $\Omega_{\hat{\rho}_{\min}}$. If $x(t_k) \in \Omega_{\hat{\rho}_{\min}}$, then activation of Eq 45 ensures that the closed-loop state remains in $\Omega_{\hat{\rho}_{\min}}$ by Eq 61 for the reasons noted in the proof of ultimate boundedness of the closed-loop state in $\Omega_{\hat{\rho}_{\min}}$ for Theorem 1.

Part 2. When $\delta_4 = 1$, the constraint of Eq 45 is again activated if $|x_i(t_k)| \geq \gamma_i$, $i = 1, \dots, n_f$, and Eq 86 holds, giving the result that repeated activation of this constraint will move the closed-loop state into $\Omega_{\hat{\rho}_{\min}}$ in t_h time units, or at least $\lfloor \frac{t_h}{\Delta} + 1 \rfloor$

sampling periods, as demonstrated in *Part 1*. If the region where $|x_i(t_k)| < \gamma_i, i = 1, \dots, n_f$ contains $\Omega_{\hat{\rho}_{\min}}$, then in a worst-case scenario, the first time that the closed-loop state enters the region where $|x_i(t_k)| < \gamma_i, i = 1, \dots, n_f$, is when it reaches the boundary of $\Omega_{\hat{\rho}_{\min}}$. Because it is guaranteed to enter $\Omega_{\hat{\rho}_{\min}}$ in t_h time units, the closed-loop state is therefore also guaranteed to enter the region where $|x_i(t_k)| < \gamma_i, i = 1, \dots, n_f$, in t_h time units.

In the following theorem, the conditions under which it is possible to switch the model for the LEMPC of Eqs 39–45 while maintaining feasibility and closed-loop stability are characterized.

Theorem 3. *Consider the closed-loop system of Eq 1 under the LEMPC of Eqs 39–45 with h_{NL} meeting Eqs 10–13, where the conditions of Theorem 1 are satisfied, where it is desired to update the LEMPC of Eqs 39–45 to replace $f_{NL}, h_{NL}, \hat{V}, \hat{\rho}, \hat{\rho}_e$, and $\hat{\rho}_{\min}$ with $f'_{NL}, h'_{NL}, \hat{V}', \hat{\rho}', \hat{\rho}'_e$, and $\hat{\rho}'_{\min}$ at t_s , where Eqs 10–13 and the conditions of Theorem 1 are satisfied by the updated parameters and functions, and $f'_{NL}(0,0) = 0$. If the update to the LEMPC of Eqs 39–45 is made when $x(t_k) \in \Omega_{\hat{\rho}_{\min}}$, and if $\Omega_{\hat{\rho}'_{\min}} \subset \Omega_{\hat{\rho}}$ and $\Omega_{\hat{\rho}_{\min}} \subset \Omega_{\hat{\rho}'}$, then closed-loop stability and recursive feasibility of the LEMPC are guaranteed both before and after the LEMPC formulation is updated. Furthermore, if $t_s \geq t' + t_h$, where t_h is defined in Theorem 2, then the closed-loop state is driven into $\Omega_{\hat{\rho}'_{\min}}$ by t_s and the LEMPC of Eqs 39–45 can be updated at t_s while maintaining closed-loop stability and recursive feasibility.*

Proof. If $\Omega_{\hat{\rho}_{\min}}$ is defined as in Eq 61, the closed-loop state is guaranteed to be driven into this region in finite time after t' (as demonstrated in the proof of Theorem 1), and specifically within t_h time units after t' (as follows from the proof of Theorem 2). Therefore, if $t_s \geq t' + t_h, x(t_s) \in \Omega_{\hat{\rho}_{\min}}$. For $t_k < t_s, x(t_k) \in \Omega_{\hat{\rho}}$ because the conditions of Theorem 1 are met by the LEMPC of Eqs 39–45 utilizing f_{NL} and the associated functions and parameters. Closed-loop stability and recursive feasibility then follow from Theorem 1. When $t_k = t_s, x(t_s) \in \Omega_{\hat{\rho}_{\min}}$, which is a subset of both $\Omega_{\hat{\rho}}$ (such that the LEMPC of Eqs 39–45 was feasible and maintained closed-loop stability until t_s) and also of $\Omega_{\hat{\rho}'}$ (such that the updated LEMPC of Eqs 39–45 is also feasible and maintains closed-loop stability of the process of Eq 1 at t_s and after from Theorem 1 applied to the updated LEMPC).

Remark 7. The conditions of Theorem 1 requiring satisfaction of Eqs 60–62 and 71–73 by $\hat{\rho}, \hat{\rho}_e, \hat{\rho}_s, \hat{\rho}_{\min}, \Delta, \Theta$, and M_{err} imply that these parameters must be sufficiently small with respect to one another such that all of the equations can be satisfied simultaneously. For example, from Eq 60, Δ has to be sufficiently small such that the positive term $L_L M_L \Delta$ does not overwhelm the negative term $-\hat{\alpha}_3(\hat{\alpha}_2^{-1}(\hat{\rho}_s))$, because, overall, it is required that the left-hand side of Eq 60 be negative for that inequality to hold. Furthermore, the value of $\hat{\rho}_s$ needs to be sufficiently small according to Eq 61 such that for a chosen $\hat{\rho}_{\min}$, which must be smaller than a desired value of $\hat{\rho}_e$, Eq 61 holds. This indicates that the sizes of these various parameters must be sufficiently small with respect to one another in the sense that as one of them is made larger or smaller, the others have to adjust as well to ensure that Eqs 60–62 and 71–73 are all simultaneously satisfied. Furthermore, for any parameters that appear in multiple equations, all equations must be met simultaneously, such that the most conservative value of the parameters among all equations (i.e., those which cause all equations to be met at once) must be chosen to obtain the theoretical results. Finally, it is significant that in Eqs 71 and 72, $\Delta, \Theta, \hat{\rho}$, and M_{err} are all required to be sufficiently small to ensure that the left-hand sides of these equations are negative. It is not guaranteed that

M_{err} for any empirical model or Θ for any disturbance scenario will cause these equations to hold. However, by obtaining more physics-based models that more closely approximate the actual underlying physics, it would be expected that M_{err} would decrease, which may make it possible to satisfy Eq 71 even when it cannot be satisfied with certain other models. Furthermore, though the first term in Eq 71 becomes more negative as $\hat{\rho}_e$ is increased, increases in $\hat{\rho}_e$ eventually necessitate increases in $\hat{\rho}$, which appears positively in the second term of Eq 71. Therefore, making $\hat{\rho}_e$ arbitrarily large is not a solution to having a larger M_{err} . In fact, as M_{err} increases, the magnitude of the second term in Eq 71 containing this term could be decreased by decreasing $\hat{\rho}$, which would require $\hat{\rho}_e$ to decrease according to Eq 72 unless it was conservatively selected. However, if M_{err} is small, the second term in Eq 71 becomes smaller even for a larger $\hat{\rho}$ and $\hat{\rho}_e$, implying that the stability region can be enlarged for fixed Δ and Θ to enhance process economic performance if M_{err} becomes smaller, which provides a significant motivation for seeking to develop more physics-based models for EMPC that would be expected to have lower M_{err} values than alternative models. Finally, from Eq 73, to obtain a small $\hat{\rho}_s$ (it is desirable to decrease Δ and $\hat{\rho}_s$, according to Eq 61 to decrease $\hat{\rho}_{min}$ and therefore guarantee that the closed-loop state of the system of Eq 1 under the LEMPC of Eqs 39–45 can be driven to a smaller neighborhood of the origin), again, M_{err} , Δ , Θ , and $\hat{\rho}$ have to be sufficiently small, where again for a fixed Δ , Θ , and $\hat{\rho}_s$, larger values of $\hat{\rho}$ can be utilized to seek to enhance process economic performance if M_{err} is smaller.

Remark 8. Refs. [32] and [31] are two works where nonlinear and linear empirical models, respectively, have been incorporated in LEMPC, and the resulting control designs are treated theoretically. Though the proof here follows in a similar fashion to the proofs in those works, an important difference is the assumptions placed on the Lyapunov-based controller for the empirical model (equivalent to h_{NL} in this work) as well as the form of the empirical model treated. Specifically, both Ref. [32] and [31] assume that the Lyapunov-based controller for the empirical system is exponentially stabilizing for that system, and this is utilized to first prove that then the Lyapunov-based controller is exponentially stabilizing for the nominal nonlinear system so that this may be used in deriving subsequent theoretical results. In the present manuscript, we require only that the Lyapunov-based controller be asymptotically stabilizing for the empirical system to allow for greater ease of investigating how the theoretical results can apply to broad classes of nonlinear empirical systems for which a Lyapunov-based controller meeting the assumptions of exponential stability may not be readily found. Furthermore, Ref. [32] assumes that the empirical model has a polynomial form, and Ref. [31] assumes that the empirical model has a linear form. This work therefore broadens the results in those articles to not require any specific form of the nonlinear model beyond the assumptions in the present manuscript to facilitate the investigation of potentially physically meaningful empirical models that do not necessarily contain only terms of a specific type.

Application to a Chemical Process Example

To demonstrate the use of an EMPC augmented with data-gathering functionality for developing or validating physics-based process models and physically relevant constraints and objective functions for the control design online, we consider an illustrative continuous stirred tank reactor (CSTR) example where an irreversible, second-order, exothermic reaction occurs. The reactant species A is converted to the product B in a reaction of the

TABLE 1

CSTR example model parameters.

Parameter	Value
T_0	300 K
V	1 m ³
k_0	$8.46 \times 10^6 \frac{\text{m}^3}{\text{hr kmol}}$
C_p	$0.231 \frac{\text{kJ}}{\text{kg K}}$
ρ_L	$1,000 \frac{\text{kg}}{\text{m}^3}$
F	$5 \frac{\text{m}^3}{\text{hr}}$
E	$5 \times 10^4 \frac{\text{kJ}}{\text{kmol}}$
ΔH	$-1.15 \times 10^4 \frac{\text{kJ}}{\text{kmol}}$
R_g	$8.314 \frac{\text{kJ}}{\text{kmol K}}$

form $A \rightarrow B$. The feed to the reactor contains the species A in an inert solvent at concentration C_{A0} and temperature T_0 . The feed volumetric flow rate is F . A jacket is used to heat/cool the reactor at heat rate Q . The density of the liquid (ρ_L), the heat capacity C_p , and the volume of the liquid V are constants with the values listed in **Table 1**. We consider that the process dynamics are described by the following dynamic model, which is derived from mass and energy balances:

$$\dot{C}_A = \frac{dC_A}{dt} = \frac{F}{V}(C_{A0} - C_A) - k_0 e^{-\frac{E}{R_g T}} C_A^2 \quad (87)$$

$$\dot{T} = \frac{dT}{dt} = \frac{F}{V}(T_0 - T) - \frac{\Delta H k_0}{\rho_L C_p} e^{-\frac{E}{R_g T}} C_A^2 + \frac{Q}{\rho_L C_p V} \quad (88)$$

$$\dot{C}_B = \frac{dC_B}{dt} = -\frac{F}{V} C_B + k_0 e^{-\frac{E}{R_g T}} C_A^2 \quad (89)$$

where C_A is the concentration of the reactant species A , T is the temperature of the reactor, and C_B is the concentration of the product species B . The reaction inside the CSTR has pre-exponential factor k_0 , enthalpy of reaction ΔH , and activation energy E . R_g represents the ideal gas constant. The manipulated inputs are C_{A0} and Q , which are constrained by actuator limitations to the following ranges: $0.5 \leq C_{A0} \leq 7.5 \frac{\text{kmol}}{\text{m}^3}$ and $-5 \times 10^5 \leq Q \leq 5 \times 10^5 \frac{\text{kJ}}{\text{hr}}$. The process will be operated around the steady-state $C_{As} = 1.22 \frac{\text{kmol}}{\text{m}^3}$, $T_s = 438.2 \text{ K}$, $C_B = 2.78 \frac{\text{kmol}}{\text{m}^3}$, $C_{A0s} = 4 \frac{\text{kmol}}{\text{m}^3}$, and $Q_s = 0 \frac{\text{kJ}}{\text{hr}}$. With these steady-state values, we can develop deviation variable vectors for the states and inputs as follows: $\bar{x} = [\bar{x}_1 \ \bar{x}_2 \ \bar{x}_3]^T = [C_A - C_{As} \ T - T_s \ C_B - C_{Bs}]^T$ and $u = [u_1 \ u_2]^T = [C_{A0} - C_{A0s} \ Q - Q_s]^T$. We consider that only C_A and T are measured and therefore we also introduce the vector of deviation variables for the measured states as follows: $x = [x_1 \ x_2] = [\bar{x}_1 \ \bar{x}_2]^T$.

The control objective is to operate the system of Eqs 87–89 in an economically optimal fashion, where the process economics are considered to be dependent on the time-averaged production rate of the product B , while respecting process constraints and maintaining closed-loop stability. These process constraints include the bounds on the two manipulated inputs. We would also like to include a constraint on the concentration of C_B in the reactor requiring the concentration of this product to be upper bounded because we consider that the product poses safety hazards and therefore we prefer to produce

it in low concentrations (specifically, we consider that we would like $C_B \leq 4.277 \frac{\text{kmol}}{\text{m}^3}$ for as much of the time of operation as possible, where this upper bound was chosen to provide a constraint that impacts the closed-loop state trajectories computed under an EMPC containing this constraint, as will be demonstrated in what follows).

We consider that we do not know ΔH or the form or parameters of the reaction rate law in Eqs 87–89 (though we consider that we have used chemical engineering judgment to postulate the form of the other terms in this model and to measure T_0 , V , C_p , ρ_L , and F). Because we do not know key terms and parameters in the first-principles model, we must initially control the process using an alternative model in the control design. We assume that standard industrial techniques for obtaining adequate data for developing a linear empirical model for control design have been performed, and that the following continuous-time linear empirical model from Ref. [31] has been developed:

$$\dot{x}_1 = -34.5x_1 - 0.473x_2 + 5.24u_1 - 8.09 \times 10^{-6}u_2 \quad (90)$$

$$\dot{x}_2 = 1,430x_1 + 18.1x_2 - 11.6u_1 + 4.57 \times 10^{-3}u_2 \quad (91)$$

To seek to maintain closed-loop stability, Lyapunov-based stability constraints will be added to the EMPC. Because of the lack of availability of the process model of Eqs 87–89, we will develop the Lyapunov-based stability constraints based on the model of Eqs 90 and 91. Specifically, we utilize the Lyapunov function $\hat{V} = x^T P x$ from Ref. [31], where the matrix P is as follows:

$$\begin{bmatrix} 1,060 & 22 \\ 22 & 0.52 \end{bmatrix} \quad (92)$$

We define $\tilde{f} = [\tilde{f}_1 \tilde{f}_2]^T$, where \tilde{f}_1 and \tilde{f}_2 are the terms in Eqs 90 and 91, respectively, that do not contain the inputs, and $\tilde{g} = [\tilde{g}_1 \tilde{g}_2]$, where $\tilde{g}_1 = [5.24 \ -11.6]^T$ and $\tilde{g}_2 = [-8.09 \times 10^{-6} \ 4.57 \times 10^{-3}]^T$. Utilizing this notation, we consider the Lyapunov-based controller h_{NL} from Ref. [31], where $h_{NL}(x) = [h_{NL,1}(x) \ h_{NL,2}(x)]^T = [0 \ h_{NL,2}(x)]^T$, and $h_{NL,2}(x)$ is given by the following function [54]:

$$h_{NL,2}(x) = \begin{cases} -\frac{L_{\tilde{f}} \hat{V} + \sqrt{L_{\tilde{f}} \hat{V}^2 + L_{\tilde{g}_2} \hat{V}^4}}{L_{\tilde{g}_2} \hat{V}}, & \text{if } L_{\tilde{g}_2} \hat{V} \neq 0 \\ 0, & \text{if } L_{\tilde{g}_2} \hat{V} = 0 \end{cases} \quad (93)$$

where $L_{\tilde{f}} \hat{V}$ and $L_{\tilde{g}_2} \hat{V}$ signify the Lie derivatives of \hat{V} with respect to \tilde{f} and \tilde{g}_2 . Following Ref. [31], $\hat{\rho} = 64.3$ and $\hat{\rho}_e = 55$ were chosen. We assume that based on past experience with this process, we expect C_B to remain below its desired threshold value of $4.277 \frac{\text{kmol}}{\text{m}^3}$ in $\Omega_{\hat{\rho}}$. A discretization of state-space within the stability region and an assessment of the steady-state value of C_B according to Eq 89 at the discretized points indicated that the steady-state value of C_B at the various $C_A - T$ combinations tested is below $4.277 \frac{\text{kmol}}{\text{m}^3}$, indicating that the assumption that C_B would primarily be below its threshold in this region without an explicit constraint being required in the LEMPC is reasonable if C_A and T are primarily driven to steady-state values by the LEMPC over time.

A difficulty with regard to the design of an LEMPC based on the information assumed to be available for the control design is that though the time-averaged production rate of B

dictates the process economics, it is not measured continuously. Applying chemical engineering fundamentals, one may consider that the production rate of B is the same as the rate at which A is reacting because we consider that only one reaction occurs in the CSTR. However, we also do not know the reaction rate of A. Therefore, it is not possible to design an EMPC with an objective function that reflects the process economics based on the available information. Because of the lack of information on an equation that can adequately describe the process economics resulting from a lack of knowledge of the process model, we initially utilize the following quadratic stage cost function:

$$L_e = x^T Qx + u^T Ru \quad (94)$$

where $Q = \text{diag}(10^4, 100)$ and $R = \text{diag}(10^4, 10^{-6})$ were chosen based on the magnitudes of x_1, x_2, u_1 , and u_2 . We enforce the constraint of Eq 44 numerically by imposing it at the end of each sampling period. When Eq 45 is activated at t_k , we impose Eq 44 at the end of sampling periods 2 to N to constrain the inputs after t_k . Therefore, the initial LEMPC design is as follows:

$$\min_{u(t) \in \mathcal{S}(\Delta)} \int_{t_k}^{t_{k+N}} \hat{x}(\tau)^T Q \hat{x}(\tau) + u(\tau)^T R u(\tau) d\tau \quad (95)$$

$$\text{s.t. } \dot{\hat{x}}(t) = \tilde{f}(\hat{x}(t)) + \tilde{g}u(t) \quad (96)$$

$$\hat{x}(t_k) = x(t_k) \quad (97)$$

$$-3.5 \leq u_1(t) \leq 3.5, \forall t \in [t_k, t_{k+N}) \quad (98)$$

$$-5 \times 10^5 \leq u_2(t) \leq 5 \times 10^5, \forall t \in [t_k, t_{k+N}) \quad (99)$$

$$\begin{aligned} \hat{V}(\hat{x}(t)) \leq \hat{\rho}_e, \text{ for } t = t_q, \text{ where } q = k + 1, \dots, k + N, \text{ if } x(t_k) \in \Omega_{\hat{\rho}_e}, \\ \text{or } q = k + 2, \dots, k + N, \text{ if } x(t_k) \notin \Omega_{\hat{\rho}_e} \end{aligned} \quad (100)$$

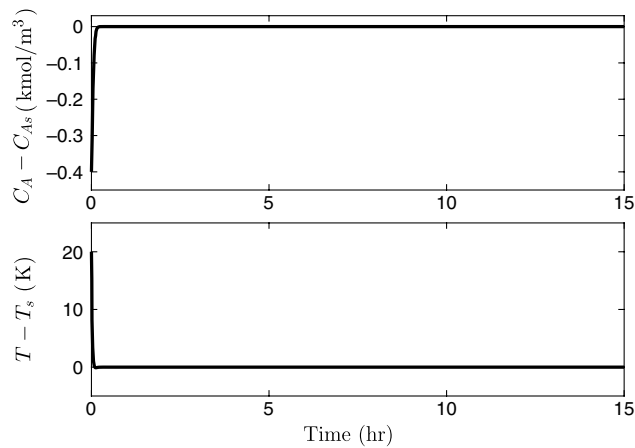
$$\begin{aligned} \frac{\partial \hat{V}(x(t_k))}{\partial \hat{x}} (\tilde{f}(x(t_k)) + \tilde{g}u(t_k)) \\ \leq \frac{\partial \hat{V}(x(t_k))}{\partial \hat{x}} (\tilde{f}(x(t_k)) + \tilde{g}h_{NL}(x(t_k))) \text{ if } x(t_k) \notin \Omega_{\hat{\rho}_e} \end{aligned} \quad (101)$$

No explicit safety-based constraint on C_B is included in this control design.

The state trajectories resulting from controlling the process of Eqs 87–89 with the LEMPC of Eqs 95–101 for 15 operating periods each of a length $t_p = 1$ hr are plotted in Fig. 1 and indicate that the LEMPC enforced steady-state operation. A prediction horizon $N = 10$ was utilized, with a sampling period $\Delta = 0.01$ hr. The empirical model of Eqs 90 and 91 was integrated within the EMPC with an integration step of 10^{-4} hr, and the first-principles model of Eqs 87 and 88 was numerically integrated with the same integration step to simulate the process to which the EMPC-computed inputs were applied. The input h_{NL} was applied without saturation at its bounds in the LEMPC or setting it to zero at the steady-state, but the inputs applied to the process were required to meet the bounds. The simulations were performed utilizing the default (interior point) solver of the MATLAB function `fmincon` in MATLAB R2016 (MathWorks, Natick, MA). Exit flags indicating that a local minimum was found or that it was possible were accepted because of the reasonableness of the closed-loop state trajectories under the resulting inputs given

FIG. 1

Profiles for x_1 and x_2 for 15 operating periods for the process of Eqs 87 and 88 operated under the LEMPC of Eqs 95–101. The initial condition for the simulations is $x_{init} = [x_{init,1} \ x_{init,2}]^T = [-0.4 \text{ kmol/m}^3 \ 20 \text{ K}]^T$, for which $V(x_{init}) = 25.6$ (i.e., the initial condition is in Ω_{pe}).



the objective function. The bounds on u_2 were divided by 10^5 to scale the problem so that u_1 and u_2 would be on more comparable orders of magnitude at their bounds. The default tolerance of `fmincon` was utilized, with the initial guess at every sampling time being the steady-state values of the inputs. The simulations were initialized from $x_1 = -0.4 \frac{\text{kmol}}{\text{m}^3}$ and $x_2 = 20 \text{ K}$ and performed using an Intel(R) Xeon(R) CPU E-3 1240 v5 at 3.50GHz (Intel, Santa Clara, CA), with 32.0 GB of memory and a 64-bit operating system with an x64-based processor running Windows 10 Enterprise (Microsoft, Redmond, WA).

We would like to update the control design online to account for process economic performance in the objective function and the desired constraint on C_B . We therefore undertake to practically design and update an EMPC online by augmenting the controller of Eqs 95–101 with data-gathering functionalities in the spirit of those described in this manuscript and utilizing techniques for extracting models from the gathered data. We first demonstrate the utility of a data-gathering LEMPC for generating nonroutine operating data that can help an engineer to detect when a model developed with the intent of it being physics-based is not correct. Specifically, we consider that the following model with an incorrect rate law form has been postulated:

$$\dot{C}_A = \frac{dC_A}{dt} = \frac{F}{V} (C_{A0} - C_A) - k_0 e^{-\frac{E}{R_g T}} \quad (102)$$

$$\dot{T} = \frac{dT}{dt} = \frac{F}{V} (T_0 - T) - \frac{\Delta H k_0}{\rho_L C_p} e^{-\frac{E}{R_g T}} + \frac{Q}{\rho_L C_p V} \quad (103)$$

where k_0 , E , and ΔH are unknown coefficients. Because this model is incorrect, it is not considered to be an improvement over Eqs 90 and 91, but rather it is a postulated model for which the data-gathering LEMPC will be used to show whether it is an acceptable or unacceptable process description.

To estimate the values of k_0 , E , and ΔH , we will, inspired by the method in Ref. [15], develop a matrix containing estimates of \dot{C}_A and \dot{T} at various times throughout the first 15 operating periods, where these estimates come from a backward finite difference approximation of the derivatives using measurements of C_A and T that are already available from

the data collected throughout the operating periods, captured every 0.0001 hr. To identify the coefficients through a linear regression, we can move terms of known value to the left-hand side of the differential equations of Eqs 102 and 103 to obtain the following system of linear algebraic equations:

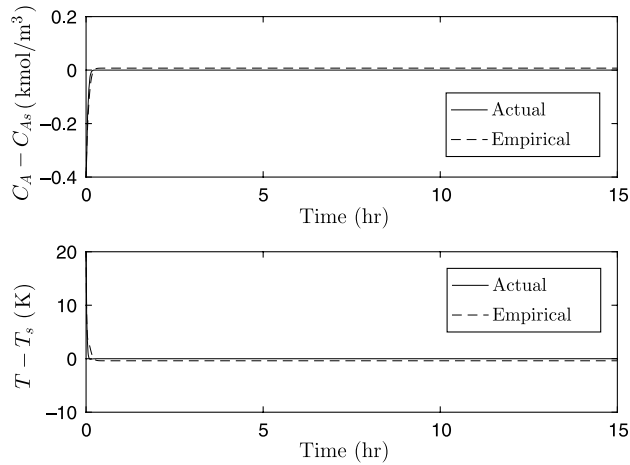
$$\begin{bmatrix} \ln(-(\dot{C}_A(\tilde{t}_1) - \frac{E}{V}(C_{A0}(\tilde{t}_1) - C_A(\tilde{t}_1)))) \\ \ln(\dot{T}(\tilde{t}_1) - \frac{E}{V}(T_0 - T(\tilde{t}_1)) - \frac{Q(\tilde{t}_1)}{\rho_L c_p V}) \\ \ln(-(\dot{C}_A(\tilde{t}_2) - \frac{E}{V}(C_{A0}(\tilde{t}_2) - C_A(\tilde{t}_2)))) \\ \ln(\dot{T}(\tilde{t}_2) - \frac{E}{V}(T_0 - T(\tilde{t}_2)) - \frac{Q(\tilde{t}_2)}{\rho_L c_p V}) \\ \vdots \\ \ln(-(\dot{C}_A(\tilde{t}_q) - \frac{E}{V}(C_{A0}(\tilde{t}_q) - C_A(\tilde{t}_q)))) \\ \ln(\dot{T}(\tilde{t}_q) - \frac{E}{V}(T_0 - T(\tilde{t}_q)) - \frac{Q(\tilde{t}_q)}{\rho_L c_p V}) \end{bmatrix} = \begin{bmatrix} 1 & 0 & \frac{1}{T(\tilde{t}_1)} \\ 1 & 1 & \frac{1}{T(\tilde{t}_1)} \\ 1 & 0 & \frac{1}{T(\tilde{t}_2)} \\ 1 & 1 & \frac{1}{T(\tilde{t}_2)} \\ \vdots & \vdots & \vdots \\ 1 & 0 & \frac{1}{T(\tilde{t}_q)} \\ 1 & 1 & \frac{1}{T(\tilde{t}_q)} \end{bmatrix} \begin{bmatrix} c_1 \\ c_2 \\ c_3 \end{bmatrix} \quad (104)$$

where the $\tilde{t}_i, i = 1, \dots, q$, represent the times corresponding to the available measurements of C_A , T , Q , and C_{A0} which are utilized in Eq 104. \tilde{t}_1 represents the first time utilized in specifying the matrices and vectors in Eq 104. The smallest possible value of \tilde{t}_1 is 0.0001 hr to account for the fact that $\dot{C}_A(t_0 = 0 \text{ hr})$ and $\dot{T}(t_0 = 0 \text{ hr})$ cannot be computed with a backward finite difference. The largest possible value of \tilde{t}_q is 14.9999 hr to account for the fact that C_{A0} and Q are computed in sample-and-hold over time intervals $[t_k, t_{k+1})$; because this interval is open, neither input has been given a value at 15 hr. The coefficients c_1 , c_2 , and c_3 correspond to $\ln(k_0)$, $\ln(-\frac{\Delta H}{\rho_L c_p})$, and $-E/R_g$ in Eqs 102 and 103. We note that because A is being consumed in the reaction, we expect $-k_0 e^{-E/(R_g T)}$ to be negative. Therefore, to allow logarithms of positive terms to be taken, we move the negative in this equation to the left-hand side of the differential equation before taking the natural logarithm. Similarly, if we calculate $(\dot{T} - \frac{E}{V}(T_0 - T) - \frac{Q}{\rho_L c_p V})$ based on the data, we would expect it to be positive, and therefore the natural logarithm of this term may be readily taken. Based on the form of the matrix in Eq 104, it can be seen that it is important to utilize data from times that do not correspond only to steady-state operation, or else the third column will contain the same number in every row, and the matrix will be singular.

Data from the first 10,001 integration steps of the 15 hrs of operation was utilized to form the matrices and vectors in Eq 104 ($q = 10,000$ to discard $\dot{C}_A(0)$ and $\dot{T}(0)$). The terms within the logarithms in Eq 104 took the expected signs (positive or negative) for these data points. The resulting system of equations was solved for c_1 , c_2 , and c_3 in MATLAB using the command “\”. This gave $c_1 = -8.6999$, $c_2 = 3.9075$, and $c_3 = 4,960.15$, which correspond to $k_0 = 0.000167 \frac{\text{m}^3}{\text{hr kmol}}$, $\Delta H = -11,498.28 \frac{\text{kJ}}{\text{kmol}}$, and $E = -41,238.71 \frac{\text{kJ}}{\text{kmol}}$. Comparing these values with those in Table 1, we can see that k_0 and E are quite far off from the true values; however, the rate law has also been guessed incorrectly, which is contributing to the mismatch. An engineer without knowledge of the true parameter values in Table 1 might check how well the identified empirical model captures the data by numerically integrating the identified process model of Eqs 102 and 103 starting from the initial condition $x_{init} = [x_{init,1} \ x_{init,2}]^T = [-0.4 \text{ kmol/m}^3 \ 20 \text{ K}]^T$ and utilizing the input trajectories computed by the EMPC for the 15 operating periods. A comparison of the data generated by the process and the predictions developed from

FIG. 2

Profiles for x_1 and x_2 measured from the process and predicted by the empirical model of Eqs 102 and 103 for 15 operating periods. The initial condition for the simulations is $x_{init} = [x_{init,1} \ x_{init,2}]^T = [-0.4 \text{ kmol/m}^3 \ 20 \text{ K}]^T$.



the empirical model are presented in Fig. 2. From this figure, it appears that the identified model provides a good fit to the data (it should be noted that changes in the data supplied to Eq 104 can have a large effect on the identified parameters [e.g., using the first 101 data points in setting up Eq 104 gives $k_0 = 40,807.98 \frac{\text{m}^3}{\text{hr kmol}}$, $\Delta H = -11,390.74 \frac{\text{kJ}}{\text{kmol}}$, and $E = 31,113.01 \frac{\text{kJ}}{\text{kmol}}$, which are very different than the values obtained with the first 10,001 data points and give significant mismatch between the simulated and plant data]).

Despite the apparent success in the model fit in Fig. 2, its prediction accuracy must still be validated with different data than has been utilized to fit the model. Therefore, we can utilize the LEMPC to obtain additional data beyond the data available under routine operation (which for this case would be more steady-state data, which we already see the model is able to fit well in Fig. 2) to aid in verifying the more physics-based process model. To introduce the desired variation in the input trajectories, we operate the process for another hour and modify the objective function of the EMPC such that in the operating period between $t = 15$ hr and $t = 16$ hr, we add one of the following terms to the stage cost at certain sampling times:

$$10^4(10,000(x_1 - x_{1,fix})^2 - 10,000(u_1 - u_1^*(t_{k-1}))^2 + (u_2 - u_2^*(t_{k-1}))^2) \quad (105)$$

$$10^4(10^{10}(x_1 - x_{1,fix})^2 - 10,000(u_1 - u_1^*(t_{k-1}))^2 + 10^{-6}(u_2 - u_2^*(t_{k-1}))^2) \quad (106)$$

where $u_1^*(t_{k-1})$ and $u_2^*(t_{k-1})$ represent the values of u_1 and u_2 implemented at the prior sampling time. The stage cost of Eq 94 with the added terms in Eqs 105 or 106 encourages the EMPC to select control actions that move x_1 toward a specified value $x_{1,fix}$ and that change the value of u_1 at each sampling time in the prediction horizon compared to its value at the prior sampling time while discouraging such changes in u_2 . The reason for this is that we want to verify whether the rate law has a zero-order dependence on C_A . We can seek to achieve this by recognizing that if the postulated rate law is correct, then changes in T should be independent of the changes in C_A and C_{A0} but should depend on Q . Therefore, if we attempt to make minimal changes in Q but more significant changes in C_A and C_{A0} ,

we would not expect T to change significantly. At the 20th, 21st, and 22nd sampling periods in the operating period between $t = 15$ hr and $t = 16$ hr, we added the term of Eq 105 to Eq 94 with $x_{1,fix} = 0.2$; at the 50th, 51st, and 52nd sampling periods in this operating period, we added the term of Eq 105 to Eq 94 with $x_{1,fix} = 0.4$; at the 60th, 61st, and 62nd sampling periods in this operating period, we added the term of Eq 106 with $x_{1,fix} = 0$; at the 90th, 91st, and 92nd sampling periods in this operating period, we added the term of Eq 105 with $x_{1,fix} = 0.2$. At sampling times besides those noted, the stage cost of Eq 94 was utilized without modifications. The results are plotted in Figs. 3–5. The data is only shown for the 16th operating period, since the prior 15 operating periods are already shown in Fig. 2. Figs. 4 and 5 present the x_2 plots from the process and from the identified empirical model of Eqs 102 and 103 against changes in the two inputs. From these figures, it

FIG. 3

Profiles for x_1 from the process and predicted by the empirical model of Eqs 102 and 103 for the 16th operating period (top plot) and for u_2 computed by the LEMPC of Eqs 95–101 with the modifications of Eqs 105 and 106 for the 16th operating period (bottom plot).

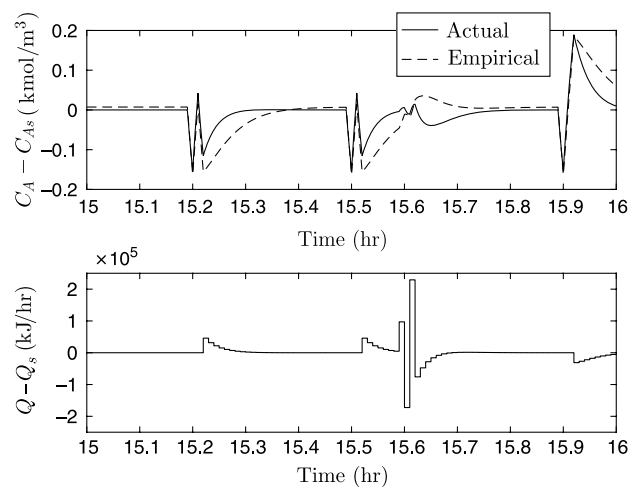


FIG. 4

Profiles for x_2 from the process and predicted by the empirical model of Eqs 102 and 103 for the 16th operating period (bottom plot) and for u_2 computed by the LEMPC of Eqs 95–101 with the modifications of Eqs 105 and 106 for the 16th operating period (top plot; the reader is referred to Fig. 3 for the full u_2 profile in the 16th operating period, but a close-up of the profile is presented here to allow more ready comparison of the times of changes in the x_2 profiles with respect to changes in u_2).

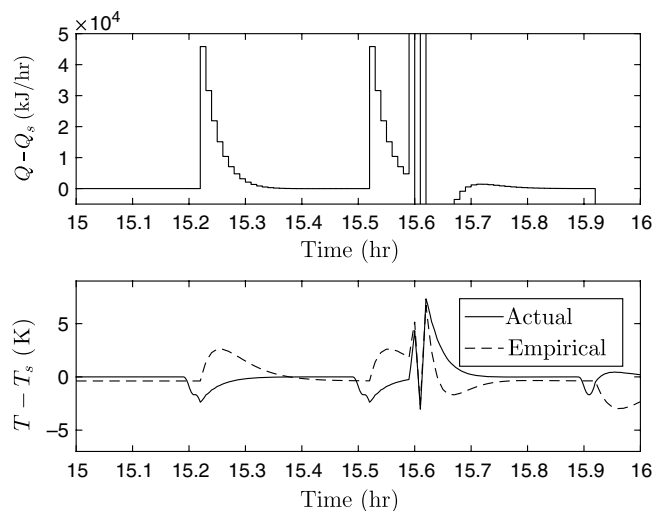
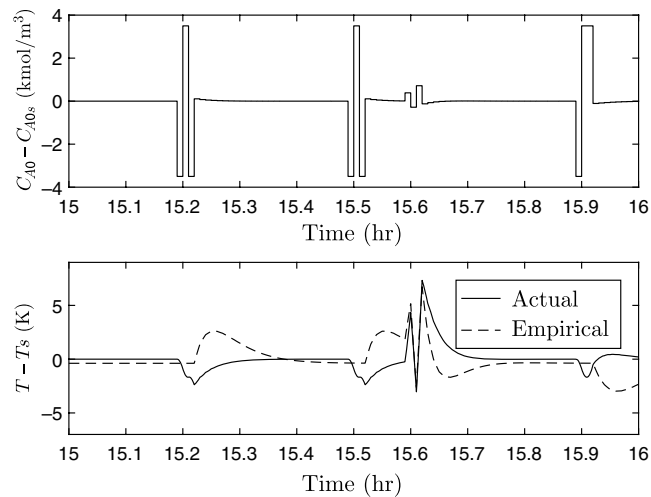


FIG. 5

Profiles for x_2 from the process and predicted by the empirical model of Eqs 102 and 103 for the 16th operating period (bottom plot) and for u_1 computed by the LEMPC of Eqs 95–101 with the modifications of Eqs 105 and 106 for the 16th operating period (top plot).



can be seen that C_{A0} seems to have an impact on x_2 , refuting the hypothesis that a physics-based model for this process has a reaction rate with a zero-order dependence on C_A . Specifically, in Fig. 4, the change in Q slightly after 15.2 hr corresponds to a change in T in the empirical model, but a change in T in the actual process begins to occur before the change in Q . A similar effect is observed slightly after 15.9 hr when Q changes, precipitating a change in T according to the empirical model; however, the value of T for the actual process begins to change before this change in Q . Fig. 5 indicates that these changes in T in the actual system that did not correspond to noticeable changes in Q may be related to changes in C_A . Based on this data, we can postulate that Eqs 102 and 103 does not contain a correct form for the rate law, and we will need to perform further analysis to develop a physics-based model to replace Eqs 90 and 91 in the LEMPC design for the process of Eqs 87–89. Specifically, Figs. 3–5 demonstrate that the rate law should contain some term indicative of changes in C_A or C_{A0} though it is not yet clear what that form should be.

In an experimental (laboratory) setting, the determination of the form of the manner in which the rate law depends on C_A could be performed [50] in a batch reactor, where the reaction rate could be measured from concentration changes over time of a reactant, and then the reaction rate could be plotted against the concentration of the reactant at each time with other variables fixed to seek to better understand the functional relationship between only the reactant concentration and the reaction rate. For the reaction at hand, we assume that we expect that C_B does not play a role given that we expect the reaction to be irreversible (so we neglect it as we seek to determine the form of the rate law), but that we expect that T and C_A may influence the reaction rate. Ideally, we would like to understand the expected type of dependence of the reaction rate on C_A and on T so that we may guess an appropriate form for the rate law and then utilize regression to determine its parameters. To do this, however, we would need to, as in the classical batch-type experiments, fix C_A while changing T to analyze the dependence of the reaction rate on temperature, and fix T while changing C_A to analyze the dependence of the reaction rate on the reactant concentration. This is another case where specific types of data have been identified as “desirable,” and we can attempt to utilize a data-gathering LEMPC to obtain this data.

Specifically, after the 16th operating period, we utilized the objective function of Eq 94 to drive the closed-loop state back to the steady-state and then replaced Eq 94 with the following stage costs at certain times over 8 hr of operation to attempt to obtain data with T fixed and C_A varying:

$$L_e = 10^4 (100(x_2 - x_{2,fix})^2) \quad (107)$$

$$L_e = 10^4 (100(x_2 - x_{2,fix})^2 + 1,000(x_1 - x_{1,fix})^2) \quad (108)$$

where $x_{2,fix} = 2.203$ and $x_{1,fix}$ was adjusted in different operating periods. Specifically, for the 18th operating period, Eq 107 was used. In the 19th, 20th, 21st, 22nd, 23rd, 24th, and 25th operating periods, Eq 108 was used with $x_{1,fix} = 0.15, 0.14, 0.13, 0.12, 0.11, 0.12,$ and $0.12,$ respectively. Fig. 6 depicts the closed-loop state trajectories over the 8 hr of operation from the 18th to the 25th operating periods and demonstrates that the LEMPC was able to approximately hold T constant over that time while C_A was varied.

After the 26th hour of operation, during which the objective function of Eq 94 was utilized, Eq 94 was replaced by the following stage costs at various times throughout the subsequent 8 hr to attempt to maintain C_A constant while varying T :

$$L_e = 10^4 (100(x_2 - x_{2,fix})^2 + 1,000(x_1 - x_{1,fix})^2) \quad (109)$$

$$L_e = 10^4 (100(x_2 - x_{2,fix})^2 + 10,000(x_1 - x_{1,fix})^2) \quad (110)$$

where $x_{1,fix} = 0.12$ and $x_{2,fix}$ was adjusted in different operating periods. Specifically, for the 27th, 28th, 29th, 30th, 31st, 32nd, 33rd, and 34th operating periods, $x_{2,fix} = 2.203, 4, 5, 2, 1, 0, -1,$ and $-2,$ respectively, and Eq 110 was utilized except in the 27th operating period in which Eq 109 was utilized. Fig. 7 depicts the closed-loop state trajectories over the 8 hr of operation from the 27th to the 34th operating periods and demonstrates that the LEMPC was able to approximately hold C_A constant over this time while T was varied.

FIG. 6

Profiles for x_1 and x_2 for the process of Eqs 87–89 for the 18th–25th operating periods under the inputs computed by the LEMPC of Eqs 95–101 with the modifications of Eqs 107 and 108.

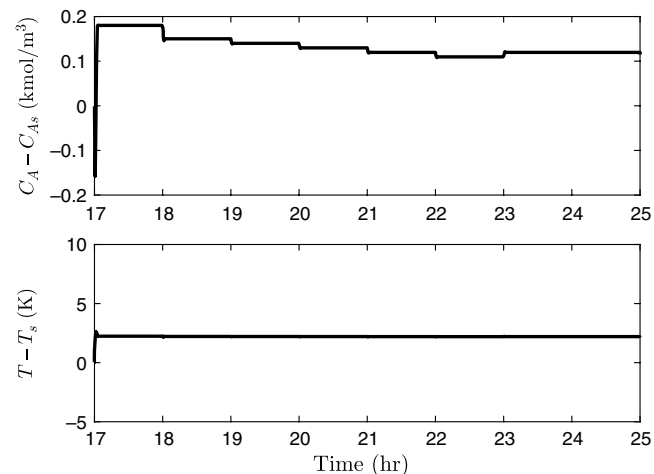
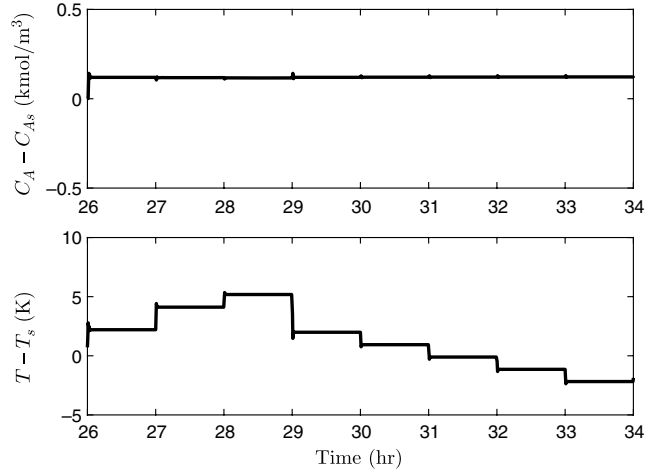


FIG. 7

Profiles for x_1 and x_2 for the process of Eqs 87–89 for the 27th–34th operating periods under the inputs computed by the LEMPC of Eqs 95–101 with the modifications of Eqs 109 and 110.



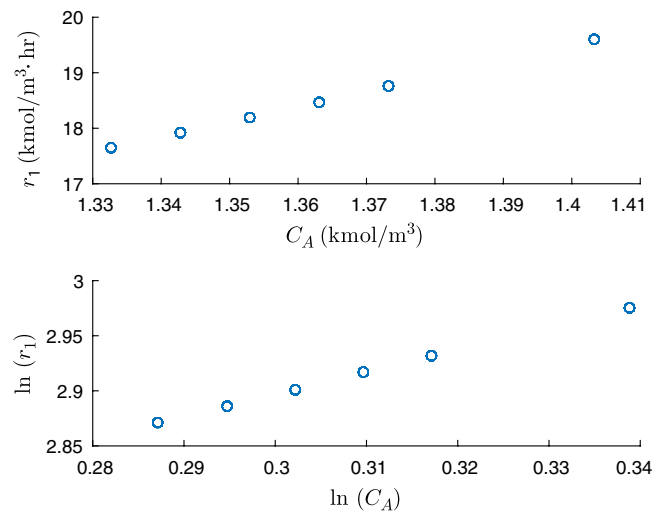
Because the controller was able to approximately achieve the desired effect of fixing one state while varying another, we can seek to develop a plot of how the reaction rate varies only with C_A and how it varies only with T to seek to propose a reasonable form of the reaction rate law expression using standard techniques for such analysis (e.g., plotting the logarithm of the reaction rate against the logarithm of C_A [50]). Regression can be utilized because a reaction rate is associated with every time that C_A and T are measured because this rate is an algebraic function of the two states. Therefore, we can solve for the reaction rate at a number of different times using a method similar to that in Eq 104. Specifically, we set up the following matrices:

$$\begin{bmatrix} \ln(-(\dot{C}_A(\tilde{t}_1) - \frac{F}{V}(C_{A0}(\tilde{t}_1) - C_A(\tilde{t}_1)))) \\ \ln(\dot{T}(\tilde{t}_1) - \frac{F}{V}(T_0 - T(\tilde{t}_1)) - \frac{Q(\tilde{t}_1)}{\rho_L c_p V}) \\ \ln(-(\dot{C}_A(\tilde{t}_2) - \frac{F}{V}(C_{A0}(\tilde{t}_2) - C_A(\tilde{t}_2)))) \\ \ln(\dot{T}(\tilde{t}_2) - \frac{F}{V}(T_0 - T(\tilde{t}_2)) - \frac{Q(\tilde{t}_2)}{\rho_L c_p V}) \\ \vdots \\ \ln(-(\dot{C}_A(\tilde{t}_q) - \frac{F}{V}(C_{A0}(\tilde{t}_q) - C_A(\tilde{t}_q)))) \\ \ln(\dot{T}(\tilde{t}_q) - \frac{F}{V}(T_0 - T(\tilde{t}_q)) - \frac{Q(\tilde{t}_q)}{\rho_L c_p V}) \end{bmatrix} = \begin{bmatrix} 0 & 1 & 0 & \cdots & 0 \\ 1 & 1 & 0 & \cdots & 0 \\ 0 & 0 & 1 & \cdots & 0 \\ 1 & 0 & 1 & \cdots & 0 \\ & & & \ddots & \\ 0 & 0 & 0 & \cdots & 1 \\ 1 & 0 & 0 & \cdots & 1 \end{bmatrix} \begin{bmatrix} c_1 \\ c_2 \\ c_3 \\ \vdots \\ c_{q+1} \end{bmatrix} \quad (111)$$

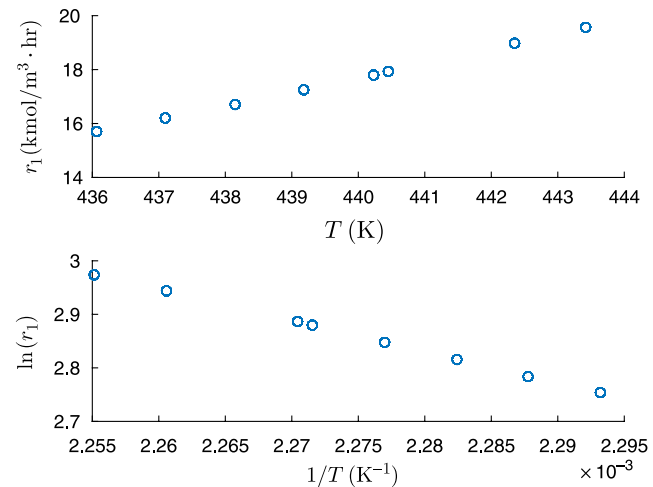
where the notation follows that in Eq 104. The coefficient c_1 corresponds to $\ln(\frac{-\Delta H}{\rho_L c_p})$, and coefficients c_2, \dots, c_{q+1} correspond to the logarithms of the reaction rates associated with each time $\tilde{t}_i, i = 1, \dots, q$ (where these reaction rates will be denoted by $r_1(\tilde{t}_i)$). The size of q used for the regression both for analyzing the dependence of r_1 on C_A and its dependence on T was 400. Fifty values of the states, inputs, and derivatives of the states were utilized from approximately halfway through each of the eight operating periods between the 18th and 25th for obtaining the C_A dependence of r_1 , and fifty values of the states, inputs, and derivatives of the states were utilized from approximately halfway through each of the

FIG. 8

Scatter plot of regression estimates of r_1 versus C_A (top plot) and of $\ln(r_1)$ versus $\ln(C_A)$ (bottom plot) for the process of Eqs 87–89 for the 18th–25th operating periods under the inputs computed by the LEMPC of Eqs 95–101 with the modifications of Eqs 107 and 108.

**FIG. 9**

Scatter plot of regression estimates of r_1 versus T (top plot) and of $\ln(r_1)$ versus $1/T$ (bottom plot) for the process of Eqs 87–89 for the 27th–34th operating periods under the inputs computed by the LEMPC of Eqs 95–101 with the modifications of Eqs 109 and 110.



eight operating periods between the 27th and 34th for obtaining the T dependence of r_1 . The scatter plots showing the variations of the regressed values of the reaction rates with temperature and concentration are plotted in Figs. 8 and 9. This information might be utilized in guessing appropriate terms in the rate law. For example, it is reasonable to postulate that there is a power of C_A in the rate law based on the linearity in a plot of $\ln(r_1)$ against $\ln(C_A)$ (Fig. 8) and that there is an exponential (Arrhenius) dependence of the reaction rate on temperature based on the linearity in a plot of $\ln(r_1)$ versus $1/T$ (Fig. 9).

Based on the analysis just performed, we can now postulate that the rate law contains a term with a form like $k_0 e^{-E/(R_s T)} C_A^d$ and perform a regression that finds the coefficients k_0 , E , and d , as well as the value of ΔH . Specifically, we set up the following matrices:

$$\begin{bmatrix} \ln(-(\dot{C}_A(\tilde{t}_1) - \frac{E}{V}(C_{A0}(\tilde{t}_1) - C_A(\tilde{t}_1)))) \\ \ln(\dot{T}(\tilde{t}_1) - \frac{E}{V}(T_0 - T(\tilde{t}_1)) - \frac{Q(\tilde{t}_1)}{\rho_L c_p V}) \\ \ln(-(\dot{C}_A(\tilde{t}_2) - \frac{E}{V}(C_{A0}(\tilde{t}_2) - C_A(\tilde{t}_2)))) \\ \ln(\dot{T}(\tilde{t}_2) - \frac{E}{V}(T_0 - T(\tilde{t}_2)) - \frac{Q(\tilde{t}_2)}{\rho_L c_p V}) \\ \vdots \\ \ln(-(\dot{C}_A(\tilde{t}_q) - \frac{E}{V}(C_{A0}(\tilde{t}_q) - C_A(\tilde{t}_q)))) \\ \ln(\dot{T}(\tilde{t}_q) - \frac{E}{V}(T_0 - T(\tilde{t}_q)) - \frac{Q(\tilde{t}_q)}{\rho_L c_p V}) \end{bmatrix} = \begin{bmatrix} 1 & \frac{1}{T(\tilde{t}_1)} & \ln(C_A(\tilde{t}_1)) & 0 \\ 1 & \frac{1}{T(\tilde{t}_1)} & \ln(C_A(\tilde{t}_1)) & 1 \\ 1 & \frac{1}{T(\tilde{t}_2)} & \ln(C_A(\tilde{t}_2)) & 0 \\ 1 & \frac{1}{T(\tilde{t}_2)} & \ln(C_A(\tilde{t}_2)) & 1 \\ \vdots & \vdots & \vdots & \vdots \\ 1 & \frac{1}{T(\tilde{t}_q)} & \ln(C_A(\tilde{t}_q)) & 0 \\ 1 & \frac{1}{T(\tilde{t}_q)} & \ln(C_A(\tilde{t}_q)) & 1 \end{bmatrix} \begin{bmatrix} c_1 \\ c_2 \\ c_3 \\ c_4 \end{bmatrix} \quad (112)$$

where the notation follows that in Eqs 104 and 111. Here, c_1 corresponds to $\ln(k_0)$, c_2 corresponds to $-E/R_g$, c_3 corresponds to d , and c_4 corresponds to $\ln(\frac{-\Delta H}{\rho_L c_p})$. In performing this regression, data from the first 9,501 integration steps was utilized (i.e., $q = 9,500$). The results estimated that $k_0 = 8,977,447.8 \frac{\text{m}^3}{\text{hr kmol}}$, $\Delta H = -11,498.19 \frac{\text{kJ}}{\text{kmol}}$, $E = 50,223.73 \frac{\text{kJ}}{\text{kmol}}$, and $d = 2.01$. The similarities between these values and those in Table 1 are notable. Also, though the rate law was not postulated to have $d = 2$ (as it is in the actual model of Eqs 87–89), $d \approx 2$ arose from the regression.

To validate this model, we utilized the data generated until this point but also some additional data generated utilizing the controller by augmenting the stage cost of Eq 94 with the following terms in the 35th operating period:

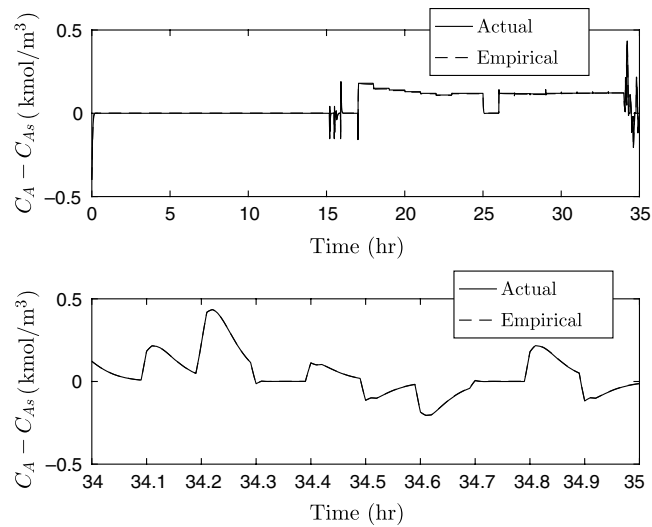
$$10^8(x_1 - x_{1,fix})^2 - 10^2(u_1 - u_1^*(t_{k-1}))^2 - 10^{-8}(u_2 - u_2^*(t_{k-1}))^2 \quad (113)$$

where $x_{1,fix} = 0.2$ for the 10th, 11th, and 12th sampling times of the 35th operating period, $x_{1,fix} = 0.4$ for the 20th, 21st, and 22nd sampling times, $x_{1,fix} = 0$ for the 30th, 31st, and 32nd sampling times, $x_{1,fix} = 0.1$ for the 40th, 41st, and 42nd sampling times, $x_{1,fix} = -0.1$ for the 50th, 51st, and 52nd sampling times, $x_{1,fix} = -0.2$ for the 60th, 61st, and 62nd sampling times, $x_{1,fix} = 0$ for the 70th, 71st, and 72nd sampling times, $x_{1,fix} = 0.2$ for the 80th, 81st, and 82nd sampling times, and $x_{1,fix} = -0.1$ for the 90th, 91st, and 92nd sampling times. Figs. 10 and 11 show the relatively good agreement between the measured data and the results generated by the identified empirical model from Eq 112 initiated from x_{init} with the same inputs as were applied to the system of Eqs 87–89 throughout the 35 operating periods, with a close-up of the results from the last operating period. The associated input trajectories are depicted in Fig. 12.

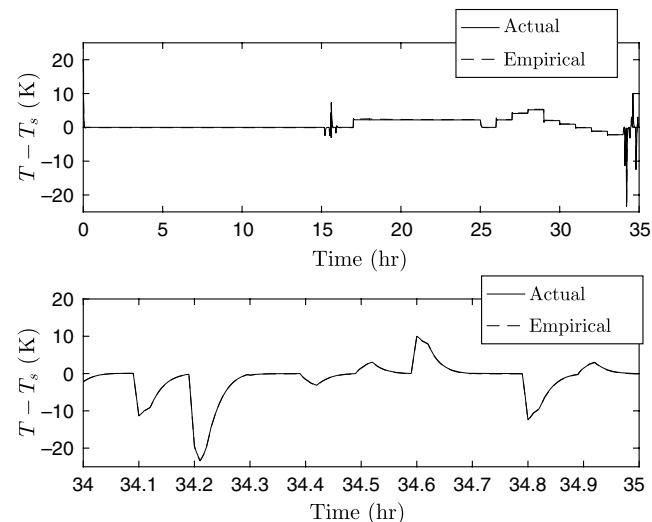
Because the newly identified model from Eq 112 is physics-based, it allows us to redesign the LEMPC online to meet our control objectives. Specifically, now that an expression for the reaction rate of A is known, this can be utilized to represent the instantaneous production rate of B, allowing us to change the objective function of the LEMPC so that it is representative of the profit of our process. Furthermore, we would like to update h_{NL} , $\hat{\rho}$, and $\hat{\rho}_e$ to enlarge the allowable region of operation based on the new model. Therefore, utilizing the nonlinear empirical model from Eq 112, we analyze the regions in state-space where a controller of the form $h'_{NL} = [0 \ h'_{NL,2}(x)]^T$, with $h'_{NL,2}(x)$ determined from Eq 93 with respect to the model from Eq 112 and saturating at the input constraints, renders \dot{V} negative along the closed-loop state trajectories of the empirical system. To do

FIG. 10

Profiles for x_1 from the process and predicted by the empirical model from Eq 112 throughout the 35 operating periods (top plot) and with a close-up of the results throughout the 35th operating period (bottom plot; the empirical model results almost overlay the process data).

**FIG. 11**

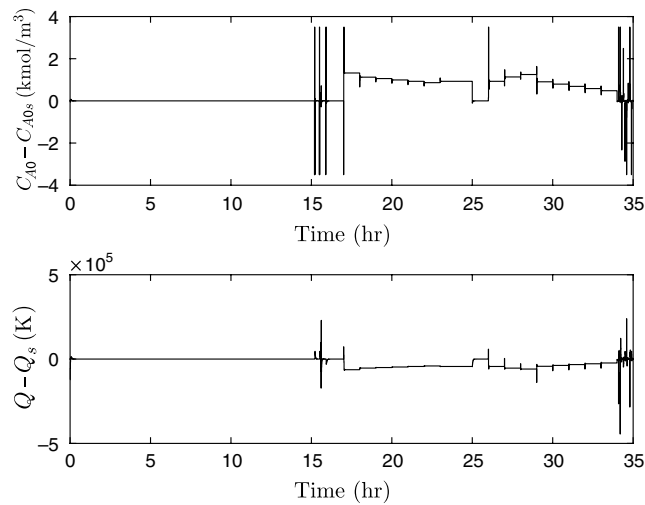
Profiles for x_2 from the process and predicted by the empirical model from Eq 112 throughout the 35 operating periods (top plot) and with a close-up of the results throughout the 35th operating period (bottom plot; the empirical model results almost overlay the process data).



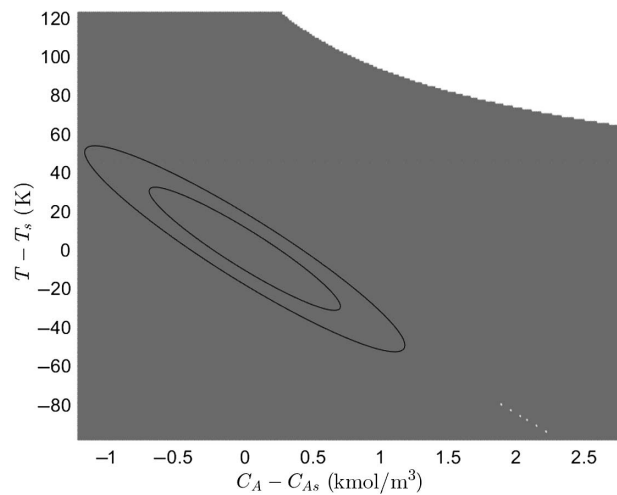
this, the C_A values between 0 kmol/m³ and 4 kmol/m³ were discretized in increments of 0.01 kmol/m³, and the T values between 340 K and 560 K were discretized in increments of 1 K. For every combination of C_A and T at the discretized points, the value of \dot{V} was checked under \bar{h}'_{NL} . Fig. 13 shows the discretized region, with the points where \dot{V} is negative in gray, and the points where it is non-negative in white. Two stability regions in the region where \dot{V} is negative are also presented—the smaller region has an upper bound on \hat{V} of 64.3 (i.e., $\hat{\rho}$), whereas the larger has an upper bound of 180 ($\hat{\rho}'$). For simplicity, we have not changed \hat{V} , though for an online process, changing \hat{V} could also be examined for attempting to enlarge the region of state-space in which time-varying operation is

FIG. 12

Profiles for u_1 (top plot) and u_2 (bottom plot) throughout the 35 operating periods.

**FIG. 13**

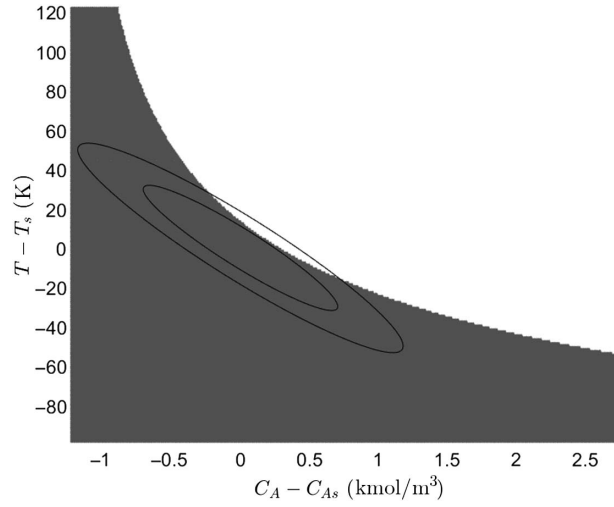
Plot showing locations in state-space where \dot{V} is negative under the controller h'_{NL} (gray points), as well as locations where it is non-negative (white points), as computed using the empirical model from Eq 112. The smaller of the two ellipses plotted represents $\Omega_{\hat{\rho}}$, whereas the larger represents $\Omega_{\hat{\rho}'}$.



allowable even further. Because the updated empirical model is unlikely to be fully accurate, some conservatism in selecting the stability region may still be warranted. The value of $\hat{\rho}'_e$ (140) selected is about 78% of the value of $\hat{\rho}'$ (though this rather *ad hoc* selection of the value of $\hat{\rho}'_e$ does not necessarily produce the theoretical guarantees described in the section titled “Data-Gathering LEMPC Stability Analysis”). Because the updated stability region allows the closed-loop state to operate in a larger region of state-space, it is important to ensure that the safety consideration with respect to C_B is accounted for in the EMPC. Because we have identified the reaction rate and expect, from chemical engineering first-principles modeling, that the equation for C_B includes $\frac{r}{V} C_B$ and the reaction rate, we are able to develop a dynamic equation for C_B to utilize within the LEMPC to enable us to then constrain this quantity (i.e., it has the form of Eq 89 but with the parameters identified

FIG. 14

Steady-state values of $C_B - C_{Bs}$ at a variety of state-space points. Points where $C_B - C_{Bs} \leq 1.5 \text{ kmol/m}^3$ are shown in gray, whereas points where $C_B - C_{Bs} > 1.5 \text{ kmol/m}^3$ are shown in white.



from Eq 112). Fig. 14 shows the regions where the steady-state value of C_B is within its desired bound at the various values of T and C_A corresponding to the discretized points described previously but where the steady-state value is computed utilizing the actual process model (i.e., the parameters of Table 1). The figure indicates that accounting for the constraint on C_B is important in $\Omega_{\rho'}$. It is significant that though C_B is still not measured, we have been able to utilize the LEMPC to develop a physics-based model that helps us to add constraints on unmeasured states to the controller to seek to enhance process operational safety.

Incorporating the previous considerations, the updated LEMPC formulation is as follows:

$$\min_{u(t) \in S(\Delta)} \int_{t_k}^{t_{k+N}} k_0 e^{-E/(R(\hat{x}_2(\tau) + T_s))} (\hat{x}_1(\tau) + C_{As})^2 d\tau \quad (114)$$

$$\text{s.t. } \dot{\hat{x}} = f'_{NL}(\hat{x}(t), u(t)) \quad (115)$$

$$\hat{x}_i(t_k) = x_i(t_k), i = 1, 2 \quad (116)$$

$$\hat{x}_3(t_k) = \tilde{x}_3(t_k) \quad (117)$$

$$-3.5 \leq u_1(t) \leq 3.5, \forall t \in [t_k, t_{k+N}) \quad (118)$$

$$-5 \times 10^5 \leq u_2(t) \leq 5 \times 10^5, \forall t \in [t_k, t_{k+N}) \quad (119)$$

$$\hat{x}_3(t) \leq 1.5, \forall t \in [t_k, t_{k+N}) \quad (120)$$

$$\begin{aligned} \dot{V}(\hat{x}(t)) &\leq \hat{\rho}_e', \text{ for } t \in [t_k, t_{k+N}), \text{ if } x(t_k) \in \Omega_{\rho_e}', \\ &\text{or } t \in [t_{k+1}, t_{k+N}), \text{ if } x(t_k) \notin \Omega_{\rho_e}', \end{aligned} \quad (121)$$

$$\begin{aligned} & \frac{\partial \hat{V}(x(t_k))}{\partial \hat{x}} f'_{NL}(x(t_k), u(t_k)) \\ & \leq \frac{\partial \hat{V}(x(t_k))}{\partial \hat{x}} f'_{NL}(x(t_k), h_{NL}(x(t_k))) \text{ if } x(t_k) \notin \Omega_{\rho'_i} \end{aligned} \quad (122)$$

where $f'_{NL}(\hat{x}, u)$ represents the physics-based model with the form of Eqs 87–89 but with parameters derived from Eq 112 (the parameters in Eq 114 are similarly derived from Eq 112), and $f'_{NL}(\hat{x}, u)$ represents this physics-based model but only with Eqs 87 and 88 because the Lyapunov-based constraints of this system are derived based only on T and C_A (from the form of Eq 89, driving C_A and T to a steady-state value also drives C_B to a steady-state value). h'_{NL} was not saturated in the constraint of Eq 122. The constraints of Eqs 120 and 121 were enforced at the end of every integration step in the time periods over which the constraints were applied. \tilde{x}_3 represents an estimate of \bar{x}_3 utilized to set the initial condition for \hat{x}_3 in Eq 115. The method by which this estimate was obtained will be further clarified in what follows. Again, the optimization problem was solved using the default solver of `fmincon`, the bounds on u_2 scaled by 10^5 , $N = 10$, $\Delta = 0.01$, and an integration step of 10^{-4} hr to simulate the model of Eq 115 and the process of Eqs 87–89. The maximum number of iterations and function evaluations allowed by MATLAB was increased in the operating period during which the LEMPC of Eqs 114–122 was used so that the solution to the optimization problem at each sampling time was stated by `fmincon` to be either a local minimum or to possibly be a local minimum. The initial guess for `fmincon` was the solution for each decision variable from the prior sampling period, except for the last sampling period of the prediction horizon in which no corresponding solution was available from the prior sampling period so that the steady-state values of u_1 and u_2 were used.

The state and input trajectories resulting from switching the LEMPC design from that of Eqs 95–101 to Eqs 114–122 for the 37th operating period are presented in Figs. 15 and 16. Specifically, in the 36th operating period, the LEMPC of Eqs 95–101 is utilized to drive the closed-loop state to the steady-state before the model is switched. Then, at the beginning of the 37th operating period, the LEMPC is changed to the design of Eqs 114–122,

FIG. 15

Profiles for x_1 and x_2 for the process of Eqs 87–89 for the 37th operating period under the inputs computed by the LEMPC of Eqs 114–122.

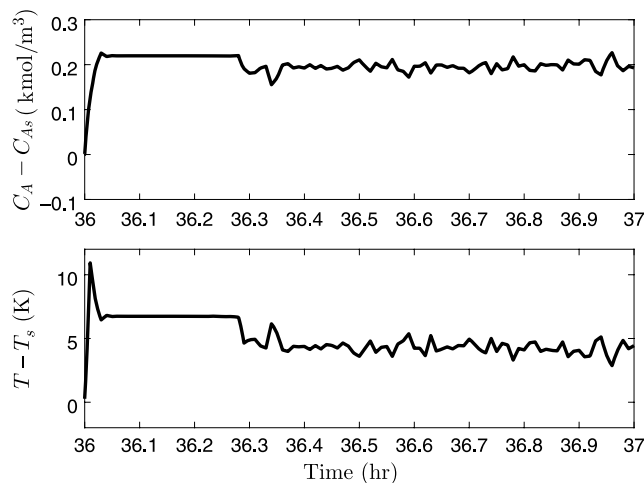
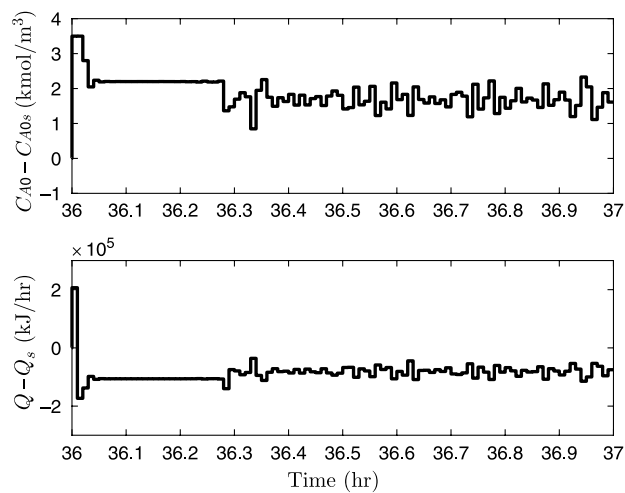


FIG. 16

Profiles for u_1 and u_2 for the process of Eqs 87–89 for the 37th operating period computed by the LEMPC of Eqs 114–122.



and the process is operated under the resulting LEMPC for a subsequent operating period. To enforce the constraint on the unmeasured state \bar{x}_3 in Eqs 114–122, the value of \bar{x}_3 was assumed to be zero at the beginning of the 37th operating period because the process had been driven to the operating steady-state in the 36th operating period. The assumed model of Eqs 87–89 with the parameters from Eq 112 was numerically integrated between sampling periods using control actions returned by the EMPC for the first sampling period of the prediction horizon to develop the estimate $\tilde{x}_3(t_k)$ at every sampling time in Eqs 114–122 (i.e., no feedback was truly available for this state at any time). However, the value of C_B was also simulated over time using Eqs 87–89 with the parameter values in Table 1 for comparison with the estimates, initialized at 2.289 kmol/m^3 at t_0 . Fig. 17 shows the bound on $C_B - C_{Bs}$, as well as the predicted and actual values of C_B during the 37th operating period. It indicates that the estimates of C_B developed from the

FIG. 17

Profiles for the actual value of $C_B - C_{Bs}$ (developed from the model of Eqs 87–89 with the parameters in Table 1 and denoted by \bar{x}_3 in the figure) and for the estimated value of $C_B - C_{Bs}$ (developed from the model of Eqs 87–89 with the parameters from Eq 112 and denoted by \tilde{x}_3 in the figure). The upper bound of $1.5 \frac{\text{kmol}}{\text{m}^3}$ on $C_B - C_{Bs}$ is denoted by $x_{3,\text{max}}$ in the figure.

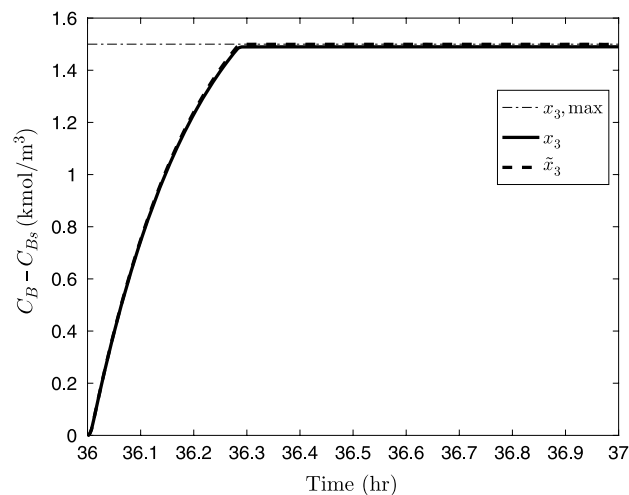
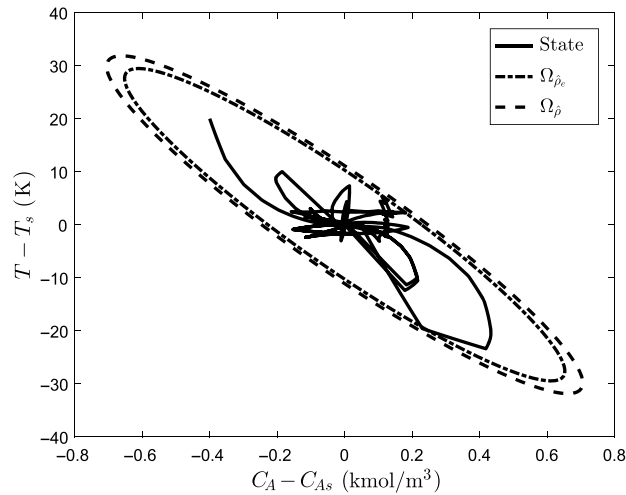
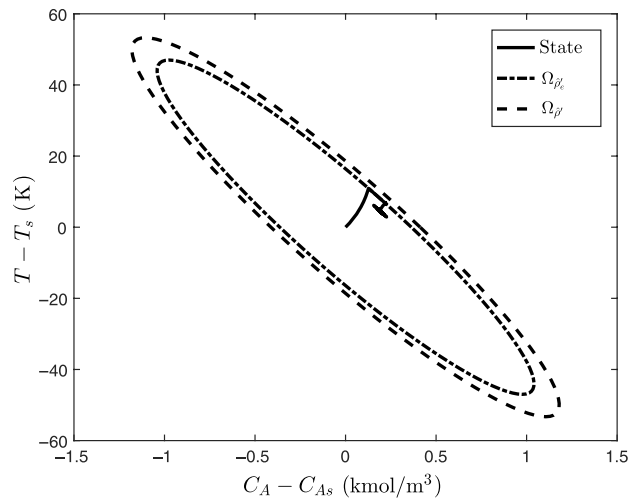


FIG. 18

$C_A - T$ trajectory in state-space for the system of Eqs 87–89 with the parameters of Table 1 throughout the first 36 operating periods (i.e., under the inputs computed by the LEMPC of Eqs 95–101 with the modifications to Eq 95 according to Eqs 105–110 and 113) with respect to $\Omega_{\hat{p}}$ and $\Omega_{\hat{p}_c}$.

**FIG. 19**

$C_A - T$ trajectory in state-space for the system of Eqs 87–89 with the parameters of Table 1 throughout the 37th operating period (i.e., under the inputs computed by the LEMPC of Eqs 114–122) with respect to $\Omega_{\hat{p}'}$ and $\Omega_{\hat{p}'_c}$.



empirical model did well at approximating the actual value of C_B and that the LEMPC of Eqs 114–122 was able to prevent C_B from going above its threshold value through the constraint of Eq 120. Furthermore, Figs. 18 and 19 show the state-space profiles for the system of Eqs 87–89 (parameters in Table 1) over the 37 periods of operation. Specifically, Fig. 18 shows the state-space profiles for the first 36 operating periods with respect to $\Omega_{\hat{p}}$ and $\Omega_{\hat{p}_c}$, while Fig. 19 shows the profiles for the last operating period with respect to $\Omega_{\hat{p}'}$ and $\Omega_{\hat{p}'_c}$. These figures indicate that both the LEMPC of Eqs 95–101 and the LEMPC of Eqs 114–122 computed input trajectories that maintained the closed-loop state within $\Omega_{\hat{p}}$ and $\Omega_{\hat{p}'}$ as applicable based on the constraints of the given operating period.

The following profit measure was assessed for the process operated under the LEMPC of Eqs 114–122 and for steady-state operation:

$$J_e = \frac{1}{t_p} \int_{36 \text{ hr}}^{37 \text{ hr}} k_0 e^{-E/(R_g T(\tau))} (C_A(\tau))^2 d\tau \quad (123)$$

where the parameters are those in **Table 1**. The value for the closed-loop process under the LEMPC was 21.98, while for the process operated at steady-state, it was 13.88, indicating that developing a physics-based empirical model online to enable the objective function to be related to the production rate of the product as desired based on the process economics, rather than retaining the original objective function of Eq 94 that enforced steady-state operation, was able to enhance the process economics for the last operating period.

Despite the success observed in the specific simulations discussed, many challenges remain to be addressed for the presented methodology. One challenge is the difficulty of seeking to find the forms of the terms to be included in a physics-based model when these terms may depend on unmeasured states. In cases where, for example, the reaction rate depends on an unmeasured state, more work needs to be performed to analyze how an engineer might guess whether the reaction rate depends on the unmeasured state, and if so, how (e.g., is the dependence through the denominator, or numerator, or both). A benefit of the data-gathering EMPC, however, is that the controller can be utilized to test the final derived physics-based model once it is obtained, which can provide greater confidence in the model if the data is fit well for a variety of different inputs, even if some assumptions are used when deriving the model. In the example, we assumed that we had measured a number of the parameters (e.g., F , V) so that we could easily place the model in the form of a linear regression with some tweaking to the form of the equations. Further work must be performed to better analyze how the nonlinear models that appear in chemical engineering might be identified without requiring so many parameters to be known *a priori*. So far also, we have required good engineering judgment in selecting the majority of the terms of the model. Ideally, the controller combined with methods for obtaining models from data would be able to also bring out terms in the model that perhaps an engineer is not aware exist in the physics of the process. It should also be able to develop models that recognize well-established constraints from physics and chemical engineering (e.g., conservation of mass and energy [14,55]).

Another challenge is the lack of ability to design a controller like LEMPC in the traditional manner when the process model is unknown. In the literature, it is traditional [28] to suggest that $\hat{\rho}_e$ be designed with respect to $\hat{\rho}$ utilizing closed-loop simulations that test a variety of scenarios with disturbances and inputs within the bounds to attempt to select a $\hat{\rho}_e$ that is expected to ensure that the closed-loop state is maintained within $\Omega_{\hat{\rho}}$ even in the presence of these disturbances and with the sample-and-hold implementation of the inputs. However, when no process model is available except the empirical model, it is not obvious how one could design a reliable closed-loop simulation technique to evaluate an adequate value of $\hat{\rho}_e$. This was reinforced by Theorem 1, where it was seen that the error between the actual and empirical models, which it is not straightforward to know, dictates the size of $\hat{\rho}_e$. This indicates that developing techniques or control designs for obtaining guaranteed closed-loop stability from an explicitly characterizable region of state-space with robustness to disturbances, but when the actual process model is not known, is important to address to enable next-generation manufacturing and, in particular, the online implementation and development of EMPC in a reliable manner. This can be particularly important when trying to develop methods for obtaining physics-based models online, as the plant-model mismatch may contribute to feasible inputs being selected that drive the

closed-loop state out of the stability region, and when performing the experiments and therefore generating nonroutine operating situations, it may be difficult to tell what types of objective functions or other changes to the LEMPC design for the purpose of experimentation might lead to such problematic inputs being generated.

It should also be noted that the objective functions utilized in this example for data-gathering purposes were obtained through extensive trial-and-error. It is not necessarily obvious how to weight the various terms added to the objective function to aid in gathering data with respect to one another to achieve effects like forcing one variable to be constant while another moves, or preventing the control actions generated from driving the closed-loop state out of Ω_{β} . Therefore, though the example suggests that if a well-designed tuning for an LEMPC could be developed, it might give desirable results, it can be difficult to obtain such a desirable tuning in practice. More work must be done to try to develop reliable methods for generating desirable types of data online that retain the simplicity of the suggested method but that also alleviate the tuning difficulties.

Another practical challenge that remains open for future work is the issue of how to determine what experiments to perform, when, and for how long. The method presented in this example takes an engineer's intuition to determine the next steps to perform in order to obtain or validate a model. Ideally, the process of obtaining physics-based models should be automated like current model identification methods that do not require a physics-based model to be identified can be. Furthermore, running experiments online throughout many hours of operation as in this example might be undesirable unless it does not cause off-specification product to be produced throughout that time period. Ideally, a strategy would be developed where the experiments could be performed in a manner that allows the process to continuously produce on-specification product throughout their duration, but also avoids having changes in the underlying dynamics before the full model is identified. Additionally, disturbances must be looked at in the context of this method. As demonstrated in the section titled "Data-Gathering LEMPC Stability Analysis," the LEMPC itself is robust to sufficiently small disturbances; however, how these affect the fidelity of the data for the model identification and therefore how to handle such effects within the context of the data-gathering EMPC implementation strategy needs further investigation. Finally, the details of the implementation of the proposed methodology in the context of a larger-scale process remain to be examined.

Remark 9. Though the theoretical results of this work require $f_{NL}(0,0)=f(0,0,0)=0$, in practice, one might identify a physics-based model that does not have exactly the same steady-state as the actual model for a given set of steady-state input values. Though the theoretical results would not rigorously hold then as written in this work, the EMPC designs in this work could still be utilized.

Remark 10. Though the use of linear regression based on approximations of derivatives for obtaining the parameters in the example was originally inspired by Ref. [15], the present work uses a data-gathering EMPC to seek to obtain enough information before performing the regression to postulate the possible terms for which parameters should be identified in the regression (and then the parameters of all of them are determined), whereas Ref. [15] uses regression to attempt to identify a physically meaningful model from a large selection of available terms which are not necessarily all in the model (and therefore the coefficients of some such terms might be neglected).

Remark 11. The focus in this work is on the development of a controller that can help in picking the model form in a manner that is physically meaningful. Once a model form has been chosen, there are a variety of methods that could be utilized for seeking to fit the model parameters. One could consider, for example, seeking to estimate and adapt them online, as in Ref. [56]. Such an approach would need to be further investigated, however, because without obtaining the parameters of the model before beginning to utilize the model in control, it may be difficult to validate that the model form selected is reasonable. For example, Eqs 102 and 103 formed an incorrectly guessed model form and therefore could not capture essential physical phenomena in Figs. 3–5. Because the parameters of the model were identified before the model was implemented within the EMPC, this error in the proposed terms of the model could be caught through the generation of the non-training data and the plotting of the actual data against that predicted with the empirical model before the EMPC was updated to include a model that was fundamentally flawed from a physics perspective. If the parameters are not estimated until after the model within the EMPC is updated, it may be more difficult to determine whether the model is physically meaningful, which might make it more difficult to appropriately design constraints and the objective function of the EMPC.

Remark 12. Though a motivation for updating the stability region after the model from Eq 112 was available was to seek to enhance process profits by allowing the process state to vary within a larger region of state-space than $\Omega_{\hat{\rho}}$, no attempt was made, either when the model of Eqs 90 and 91 or the model from Eq 112 were used, to determine the largest possible region in state-space that could be utilized in an LEMPC to enhance process economic performance because this was considered secondary to the demonstration of the functionality of the data-gathering LEMPC for aiding in online EMPC design. For an actual process, it is advisable to investigate the stability region size and shape more rigorously before choosing a value, as this may impact process economic performance. A large stability region (ideally, the full null controllable region [57]) gives greater flexibility to the EMPC in optimizing the process economics. In Ref. [57], a technique is developed for generating Lyapunov functions for which the level sets are the null controllable region, which will be a larger set than any stability region generated with a technique that relies on an explicit stabilizing controller as explored in the example presented previously. An EMPC that takes advantage of such Lyapunov functions may be economically beneficial for this and other processes. For example, when $\hat{V} = 1, 200x_1^2 + 10x_1x_2 + 0.1x_2^2$, $\hat{\rho}' = 320$, $\hat{\rho}_e' = 250$, and h_{NL} is given by Eq 93 with respect to this new \hat{V} in the 37th operating period, $J_e = 22.56$, which is higher than the value reported for the 37th operating period with a different stability region, as shown previously. Therefore, modifying the stability region for this example may enhance process economic performance.

Conclusion

In this work, a new data-gathering EMPC design has been developed that activates certain hard and soft constraints for short periods of time to seek to obtain data from an online process that may be helpful in developing a physically meaningful empirical model for a process. An example formulation of a data-gathering EMPC with Lyapunov-based stability constraints was developed with guaranteed feasibility and closed-loop stability properties

under sufficient conditions. This constitutes a difference between the proposed technique and other techniques such as bump tests or set-point changes of linear controllers at a plant [22] that might be utilized to obtain data but for which closed-loop stability guarantees might not be developed. A chemical process example was used to demonstrate the potential of a data-gathering LEMPC to drive the closed-loop states to desired values that provide the data needed to suggest a model structure for an identification algorithm and to subsequently validate the model obtained while maintaining closed-loop stability.

ACKNOWLEDGMENTS

Financial support from Wayne State University is gratefully acknowledged.

References

- [1] Qin, S. J. and Badgwell, T., "A Survey of Industrial Model Predictive Control Technology," *Control Eng. Pract.*, Vol. 11, No. 7, 2003, pp. 733–764, [https://doi.org/10.1016/S0967-0661\(02\)00186-7](https://doi.org/10.1016/S0967-0661(02)00186-7)
- [2] Rawlings, J. B., "Tutorial Overview of Model Predictive Control," *IEEE Control Syst. Mag.*, Vol. 20, No. 3, 2000, pp. 38–52, <https://doi.org/10.1109/37.845037>
- [3] Mayne, D. Q., Rawlings, J. B., Rao, C. V., and Scolaert, P. O. M., "Constrained Model Predictive Control: Stability and Optimality," *Automatica*, Vol. 36, No. 6, 2000, pp. 789–814, [https://doi.org/10.1016/S0005-1098\(99\)00214-9](https://doi.org/10.1016/S0005-1098(99)00214-9)
- [4] Narasingam, A., Siddhamshetty, P., and Kwon, J. S.-I., "Handling Spatial Heterogeneity in Reservoir Parameters Using Proper Orthogonal Decomposition Based Ensemble Kalman Filter for Model-Based Feedback Control of Hydraulic Fracturing," *Ind. Eng. Chem. Res.*, Vol. 57, No. 11, 2018, pp. 3977–3989, <https://doi.org/10.1021/acs.iecr.7b04927>
- [5] Billings, S. A., *Nonlinear System Identification: NARMAX Methods in the Time, Frequency, and Spatio-Temporal Domains*, John Wiley & Sons, Hoboken, NJ, 2013, 587p.
- [6] Ljung, L., *System Identification: Theory for the User*, Prentice Hall PTR, Upper Saddle River, NJ, 1999, 609p.
- [7] van Overschee, P. and de Moor, B. L., *Subspace Identification for Linear Systems: Theory, Implementation, Applications*, Kluwer Academic Publishers, Norwell, MA, 1996, 253p.
- [8] Paduart, J., Lauwers, L., Swevers, J., Smolders, K., Schoukens, J., and Pintelon, R., "Identification of Nonlinear Systems Using Polynomial Nonlinear State Space Models," *Automatica*, Vol. 46, No. 4, 2010, pp. 647–656, <https://doi.org/10.1016/j.automatica.2010.01.001>
- [9] Favoreel, W., de Moor, B., and van Overschee, P., "Subspace State Space System Identification for Industrial Processes," *J. Process Control*, Vol. 10, Nos. 2–3, 2000, pp. 149–155, [https://doi.org/10.1016/S0959-1524\(99\)00030-X](https://doi.org/10.1016/S0959-1524(99)00030-X)
- [10] Eskinat, E., Johnson, S. H., and Luyben, W. L., "Use of Hammerstein Models in Identification of Nonlinear Systems," *AIChE J.*, Vol. 37, No. 2, 1991, pp. 255–268, <https://doi.org/10.1002/aic.690370211>
- [11] Verdult, V., "Nonlinear System Identification: A State-Space Approach," Ph.D. thesis, University of Twente, Enschede, the Netherlands, 2002.
- [12] Viberg, M., "Subspace-Based Methods for the Identification of Linear Time-Invariant Systems," *Automatica*, Vol. 31, No. 12, 1995, pp. 1835–1851, [https://doi.org/10.1016/0005-1098\(95\)00107-5](https://doi.org/10.1016/0005-1098(95)00107-5)
- [13] Verhaegen, M. and Dewilde, P., "Subspace Model Identification Part 1. The Output-Error State-Space Model Identification Class of Algorithms," *Int. J. Control*, Vol. 56, No. 5, 1992, pp. 1187–1210, <https://doi.org/10.1080/00207179208934363>

- [14] Schmidt, M. and Lipson, H., "Distilling Free-Form Natural Laws from Experimental Data," *Science*, Vol. 324, No. 5923, 2009, pp. 81–85, <https://doi.org/10.1126/science.1165893>
- [15] Brunton, S. L., Proctor, J. L., and Kutz, J. N., "Discovering Governing Equations from Data by Sparse Identification of Nonlinear Dynamical Systems," *PNAS*, Vol. 113, No. 15, 2016, pp. 3932–3937, <https://doi.org/10.1073/pnas.1517384113>
- [16] Alpaydin, E., *Introduction to Machine Learning*, The MIT Press, Cambridge, MA, 2014, 616p.
- [17] Dhar, V., "Data Science and Prediction," *Commun. of the ACM*, Vol. 56, No. 12, 2013, pp. 64–73, <https://doi.org/10.1145/2500499>
- [18] Ong, C. J., Sui, D., and Gilbert, E. G., "Enlarging the Terminal Region of Nonlinear Model Predictive Control Using the Support Vector Machine Method," *Automatica*, Vol. 42, No. 6, 2006, pp. 1011–1016, <https://doi.org/10.1016/j.automatica.2006.02.023>
- [19] Negenborn, R. R., De Schutter, B., Wiering, M. A., and Hellendoorn, H., "Learning-Based Model Predictive Control for Markov Decision Processes," presented at the *16th IFAC World Congress*, Prague, Czech Republic, July 3–8, 2005, Elsevier, New York, NY, pp. 354–359.
- [20] Piché, S., Keeler, J., Martin, G., Boe, G., Johnson, D., and Gerules, M., "Neural Network Based Model Predictive Control," presented at the *12th International Conference on Neural Information Processing Systems*, Denver, CO, Nov. 19–Dec. 4, 1999, The MIT Press, Cambridge, MA, pp. 1029–1035.
- [21] Hosen, M. A., Hussain, M. A., and Mjalli, F. S., "Control of Polystyrene Batch Reactors Using Neural Network Based Model Predictive Control (NNMPC): An Experimental Investigation," *Control Eng. Pract.*, Vol. 19, No. 5, 2011, pp. 454–467, <https://doi.org/10.1016/j.conengprac.2011.01.007>
- [22] Draeger, A., Engell, S., and Ranke, H., "Model Predictive Control Using Neural Networks," *IEEE Control Syst. Mag.*, Vol. 15, No. 5, 1995, pp. 61–66, <https://doi.org/10.1109/37.466261>
- [23] Kaiser, E., Kutz, J. N., and Brunton, S. L., "Sparse Identification of Nonlinear Dynamics for Model Predictive Control in the Low-Data Limit," *arXiv preprint arXiv:1711.05501*, 2017, <http://web.archive.org/web/20180702080731/https://arxiv.org/pdf/1711.05501.pdf>, (accessed 2 July 2018).
- [24] Sidhu, H. S., Narasingam, A., Siddhamshetty, P., and Kwon, J. S.-I., "Model Order Reduction of Nonlinear Parabolic PDE Systems with Moving Boundaries Using Sparse Proper Orthogonal Decomposition: Application to Hydraulic Fracturing," *Comput. Chem. Eng.*, Vol. 112, 2018, pp. 92–100, <https://doi.org/10.1016/j.compchemeng.2018.02.004>
- [25] Narasingam, A. and Kwon, J. S.-I., "Development of Local Dynamic Mode Decomposition with Control: Application to Model Predictive Control of Hydraulic Fracturing," *Comput. Chem. Eng.*, Vol. 106, 2017, pp. 501–511, <https://doi.org/10.1016/j.compchemeng.2017.07.002>
- [26] Davis, J., Edgar, T., Graybill, R., Korambath, P., Schott, B., Swink, D., Wang, J., and Wetzel, J., "Smart Manufacturing," *Annu. Rev. Chem. Biomol. Eng.*, Vol. 6, 2015, pp. 141–160, <https://doi.org/10.1146/annurev-chembioeng-061114-123255>
- [27] Christofides, P. D., Davis, J. F., El-Farra, N. H., Clark, D., Harris, K. R. D., and Gipson, J. N., "Smart Plant Operations: Vision, Progress and Challenges," *AIChE J.*, Vol. 53, No. 11, 2007, pp. 2734–2741, <https://doi.org/10.1002/aic.11320>
- [28] Ellis, M., Durand, H., and Christofides, P. D., "A Tutorial Review of Economic Model Predictive Control Methods," *J. Process Control*, Vol. 24, No. 8, 2014, pp. 1156–1178, <https://doi.org/10.1016/j.jprocont.2014.03.010>
- [29] Rawlings, J. B., Angeli, D., and Bates, C. N., "Fundamentals of Economic Model Predictive Control," presented at the *IEEE 51st Annual Conference on Decision and Control*, Maui, Hawaii, Dec. 10–13, 2012, IEEE, Piscataway, NJ, pp. 3851–3861.
- [30] Müller, M. A. and Allgöwer, F., "Economic and Distributed Model Predictive Control: Recent Developments in Optimization-Based Control," *SICE J. Control, Meas., Syst. Integr.*, Vol. 10, No. 2, 2017, pp. 39–52, <https://doi.org/10.9746/jcmsi.10.39>

- [31] Alanqar, A., Ellis, M., and Christofides, P. D., "Economic Model Predictive Control of Nonlinear Process Systems Using Empirical Models," *AICHE J.*, Vol. 61, No. 3, 2015, pp. 816–830, <https://doi.org/10.1002/aic.14683>
- [32] Alanqar, A., Durand, H., and Christofides, P. D., "On Identification of Well-Conditioned Nonlinear Systems: Application to Economic Model Predictive Control of Nonlinear Processes," *AICHE J.*, Vol. 61, No. 10, 2015, pp. 3353–3373, <https://doi.org/10.1002/aic.14942>
- [33] Albalawi, F., Durand, H., and Christofides, P. D., "Process Operational Safety Using Model Predictive Control Based on a Process Safeness Index," *Comput. Chem. Eng.*, Vol. 104, 2017, pp. 76–88, <https://doi.org/10.1016/j.compchemeng.2017.04.010>
- [34] Giuliani, L. and Durand, H., "Economic Model Predictive Control Design via Nonlinear Model Identification," presented at the *Sixth IFAC Conference on Nonlinear Model Predictive Control*, Madison, WI, Aug. 19–22, 2018, in press.
- [35] Kheradmandi, M. and Mhaskar, P., "Data Driven Economic Model Predictive Control," *Mathematics*, Vol. 6, No. 4, 2018, <https://doi.org/10.3390/math6040051>
- [36] Ma, J., Qin, J., Salsbury, T., and Xu, P., "Demand Reduction in Building Energy Systems Based on Economic Model Predictive Control," *Chem. Eng. Sci.*, Vol. 67, No. 1, 2012, pp. 92–100, <https://doi.org/10.1016/j.ces.2011.07.052>
- [37] Alanqar, A., Durand, H., and Christofides, P. D., "Error-Triggered On-Line Model Identification for Model-Based Feedback Control," *AICHE J.*, Vol. 63, No. 3, 2017, pp. 949–966, <https://doi.org/10.1002/aic.15430>
- [38] Alanqar, A., Durand, H., and Christofides, P. D., "Fault-Tolerant Economic Model Predictive Control Using Error-Triggered Online Model Identification," *Ind. Eng. Chem. Res.*, Vol. 56, No. 19, 2017, pp. 5652–5667, <https://doi.org/10.1021/acs.iecr.7b00576>
- [39] Heidarinejad, M., Liu, J., and Christofides, P. D., "Economic Model Predictive Control of Nonlinear Process Systems Using Lyapunov Techniques," *AICHE J.*, Vol. 58, No. 3, 2012, pp. 855–870, <https://doi.org/10.1002/aic.12672>
- [40] Xu, J. and Froment, G. F., "Methane Steam Reforming, Methanation and Water-Gas Shift: I. Intrinsic Kinetics," *AICHE J.*, Vol. 35, No. 1, 1989, pp. 88–96, <https://doi.org/10.1002/aic.690350109>
- [41] Liu, J., Chen, X., Muñoz de la Peña, D., and Christofides, P. D., "Sequential and Iterative Architectures for Distributed Model Predictive Control of Nonlinear Process Systems," *AICHE J.*, Vol. 56, No. 8, 2010, pp. 2137–2149, <https://doi.org/10.1002/aic.12155>
- [42] Wächter, A. and Biegler, L. T., "On the Implementation of an Interior-Point Filter Line-Search Algorithm for Large-Scale Nonlinear Programming," *Math. Program.*, Vol. 106, No. 1, 2006, pp. 25–57, <https://doi.org/10.1007/s10107-004-0559-y>
- [43] Müller, M. A. and Grüne, L., "Economic Model Predictive Control without Terminal Constraints for Optimal Periodic Behavior," *Automatica*, Vol. 70, 2016, pp. 128–139, <https://doi.org/10.1016/j.automatica.2016.03.024>
- [44] Diehl, M., Amrit, R., and Rawlings, J. B., "A Lyapunov Function for Economic Optimizing Model Predictive Control," *IEEE Trans. Autom. Control*, Vol. 56, No. 3, 2011, pp. 703–707, <https://doi.org/10.1109/TAC.2010.2101291>
- [45] Amrit, R., Rawlings, J. B., and Angeli, D., "Economic Optimization Using Model Predictive Control with a Terminal Cost," *Annu. Rev. Control*, Vol. 35, No. 2, 2011, pp. 178–186, <https://doi.org/10.1016/j.arcontrol.2011.10.011>
- [46] Faulwasser, T. and Bonvin, D., "On the Design of Economic NMPC Based on an Exact Turnpike Property," presented at the *Ninth IFAC Symposium on Advanced Control of Chemical Processes*, Whistler, Canada, June 7–10, 2015, Elsevier, New York, NY, pp. 525–530.
- [47] Durand, H. and Christofides, P. D., "Actuator Stiction Compensation via Model Predictive Control for Nonlinear Processes," *AICHE J.*, Vol. 62, No. 6, 2016, pp. 2004–2023, <https://doi.org/10.1002/aic.15171>

- [48] Özgülsen, F., Adomaitis, R. A., and Çınar, A., “A Numerical Method for Determining Optimal Parameter Values in Forced Periodic Operation,” *Chem. Eng. Sci.*, Vol. 47, No. 3, 1992, pp. 605–613, [https://doi.org/10.1016/0009-2509\(92\)80011-Z](https://doi.org/10.1016/0009-2509(92)80011-Z)
- [49] Brásio, A. S. R., Romanenko, A., and Fernandes, N. C. P., “Modeling, Detection and Quantification, and Compensation of Stiction in Control Loops: The State of the Art,” *Ind. Eng. Chem. Res.*, Vol. 53, No. 39, 2014, pp. 15020–15040, <https://doi.org/10.1021/ie501342y>
- [50] Fogler, H. S., *Elements of Chemical Reaction Engineering*, 4th ed., Prentice Hall, Upper Saddle River, NJ, 2005, 1080p.
- [51] Alanqar, A., Durand, H., Albalawi, F., and Christofides, P. D., “An Economic Model Predictive Control Approach to Integrated Production Management and Process Operation,” *AIChE J.*, Vol. 63, No. 6, 2017, pp. 1892–1906, <https://doi.org/10.1002/aic.15553>
- [52] Khalil, H. K., *Nonlinear Systems*, 3rd ed., Prentice Hall, Upper Saddle River, NJ, 2002, 750p.
- [53] Mhaskar, P., Liu, J., and Christofides, P. D., *Fault-Tolerant Process Control: Methods and Applications*, Springer-Verlag, London, UK, 2013, 264p.
- [54] Sontag, E. D., “A ‘Universal’ Construction of Artstein’s Theorem on Nonlinear Stabilization,” *Syst. Control Lett.*, Vol. 13, No. 2, 1989, pp. 117–123, [https://doi.org/10.1016/0167-6911\(89\)90028-5](https://doi.org/10.1016/0167-6911(89)90028-5)
- [55] Loiseau, J.-C. and Brunton, S. L., “Constrained Sparse Galerkin Regression,” *J. Fluid Mech.*, Vol. 838, 2018, pp. 42–67, <https://doi.org/10.1017/jfm.2017.823>
- [56] Das, B. and Mhaskar, P., “Adaptive Output-Feedback Lyapunov-Based Model Predictive Control of Nonlinear Process Systems,” *Int. J. Robust Nonlinear Control*, Vol. 28, No. 5, 2018, pp. 1597–1609, <https://doi.org/10.1002/rnc.3973>
- [57] Homer, T. and Mhaskar, P., “Utilizing Null Controllable Regions to Stabilize Input-Constrained Nonlinear Systems,” *Comput. Chem. Eng.*, Vol. 108, 2018, pp. 24–30, <https://doi.org/10.1016/j.compchemeng.2017.08.002>